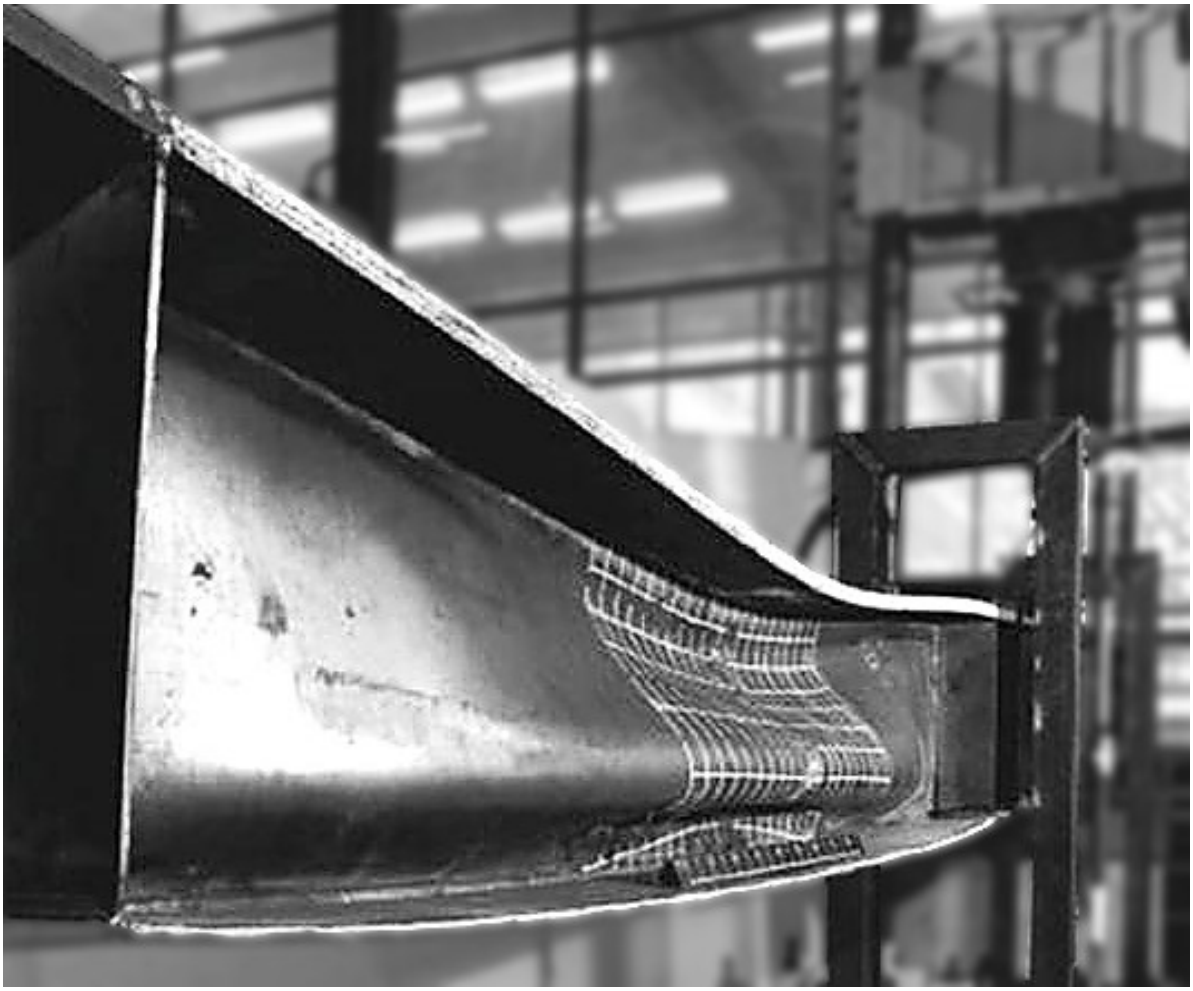

FINITE ELEMENT IMPLEMENTATION OF THE ASYMPTOTIC POSTBUCKLING MODEL

School of Engineering and Science
Aalborg University
2014

Title: Finite element implementation of the asymptotic postbuckling model

Attendees:

Daniele Della Rosa

Supervisor:
Lars Damkilde

Number of pages: 79

Number of appendices: 2

Completed: 20-08-2014

Synopsis:

The thesis deal with the Finite Element formulation of the asymptotic structural postbuckling model. At first it will be shown briefly the mathematical model based on an expansion in a perturbation series of both displacement field and load coefficient. Hence the model will be implemented in a FEM environment, and at first 2D beam element will be analyzed. The aim of the project is to show the necessary steps to carry out in order to employ a finite element analysis to characterize the postbuckling behavior of a structure through the calculation of both critical load factor and buckling coefficients. A Roodra's frame will be use as an example to show the validity of the process regarding 2-D beam elements. Later on an implementation of the asymptotic postbuckling model has been done using 3-D beam elements. A simple column/beam/column frame will be used as an example to support the implementation of the model. For both 2-D and 3-D discretization, a comparison with a non-linear analysis will be done. The non-linear analysis will be employed by means of ABAQUS while the the FE implementation, a code will be build by means of Matlab.

Preface

This project is worked out by Daniele Della Rosa in the second year of Master in Structural and Civil Engineering at the Faculty of Engineering and Science at Aalborg University. The project is designed in the period between. The overall theme is *Asymptotic post-buckling behavior*.

A special thank to supervisor Lars Damkilde for the professional training and guidance.

Reading guide

References in this project are written in Harvard method. The literature list is structured so, books will be presented with: title, author, year of publication, number and publisher. For Websites: Author, title, address and in some cases the date of the last edition. Figures, tables and formulas will be numbered, as in this example: Figure 6.2, where the 6 stands for chapter 6 and 2 stands for the second figure in Chapter 6. Tables and formulas are numbered independently. This means that there can be found Table 6.2 and Figure 6.2.

List of Figures

List of Tables

Introduction 1

When a compressive load is applied on a structure, buckling can occur and it can affect the entire structure or a component thereof.
Buckling is a sudden loss of stiffness that can compromise the functionality of the structure and can occur before yielding. Thus studying and understanding the buckling phenomenon in all its phases is necessary for a correct design of all kind of structure, from wind turbines to airplanes. When the buckling phenomenon is analyzed, it is possible to identify three main phases, shown in Fig 1.1.

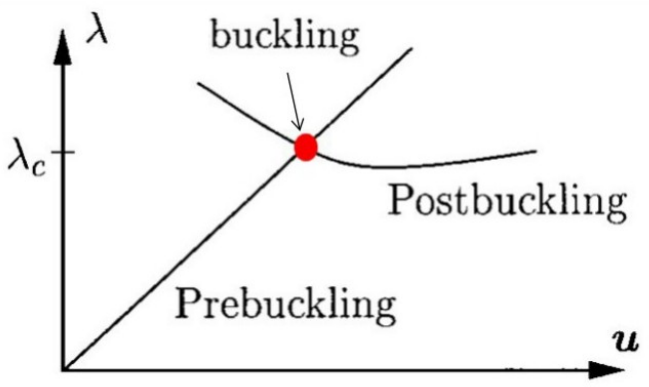

Figure 1.1. Buckling phases, [Poulsen and Damkilde, 1998]

where:

λ	Load factor
λ_c	Critical load factor
u	Displacement

All the buckling phases are specific for different kind of structures, since the buckling is strictly related not only with the geometrical and material properties of the structure, but also with its boundary conditions.
Prebuckling is the phase in which the load applied is less than the critical load, and buckling is not reached yet. The prebuckling can be linear or non-linear depending on the geometry of the analyzed structure. In the following linear prebuckling is used which

means that regarding the prebuckling phase, a stadard elastic linear analysis is employed. When the compressive load reach its critical value, buckling occur. The point where the critical load is reached, represented in Fig. 1.1 by a red dot, is also called *bifurcation point*. The buckling is a non-linear phenomenon that bring to a change in relation between the applied load and the resulting displacement. Thus is no longer possible to use common linear approximation to characterize the behavior of the structure.
Buckling, as it was previously mentioned, induce a loss of stiffness. The loss of stiffness is not equal for all kind of structure but is strictly related to the boundary conditions that are applied as it is shown in Fig. 1.2. Thus a structure can be more or less sensitive to imperfections that means the functionality of a structure can be more or less compromise due to the loss of stiffness related to the buckling phenomenon.

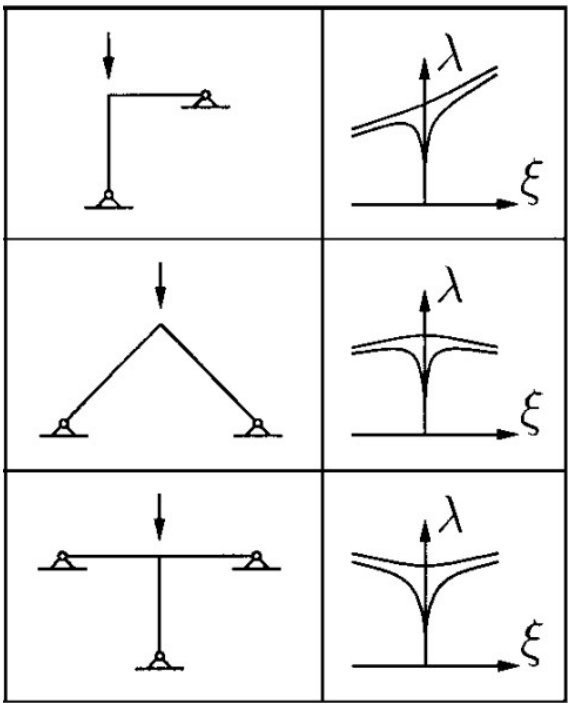

Figure 1.2. Imperfection sensitivity,[Poulsen and Damkilde, 1998]

In order to predict the stability of a buckling phenomenon and describe the imperfection sensitivity of different kind of structures, an asymptotic model has been presented by Koiter. Koiter's model consist in an analytical description of the postbuckling behavior in the neighborhood of the bifurcation point using two buckling coefficients which represent the postbuckling slope and curvature [Rahman, 2009]. According to the asymptotic postbuckling behavior model, analytical solutions for particular and simple cases have been found.
Nowadays FEM (Finite Element Method) is widely diffused in structural analysis and not only. Since buckling is a non-linear phenomenon it is necessary a full non-linear analysis to investigate buckling using commercial FE programs. Performing this kind of analysis in a preliminary design stage or in an optimization problem can be inconvenient from a computational cost point of view [Rahman, 2009]. The aim of the following thesis is to shown how to import in a FE environment the asymptotic model in order to:

- Predict and describe the postbuckling behavior of all kind of structure no matter the geometry, material and boundary conditions.
- Provide a solution that is precise enough and for which lower computational costs are needed.

In particular will be investigated the use of 2-D and 3-D beam elements together with the asymptotic postbuckling model.

Asymptotic Analysis 2

This chapter deal with the Asymptotic postbuckling behavior model and its application. At first a brief introduction on the virtual work will be done. After all the static quantities like displacement, strain and stresses fields together with the load coefficient will be describe using a perturbation series mainly depended on two buckling coefficients. The buckling coefficients will be describe using stresses and strains field related to the buckling's phases. The analytical results for a Roodra's frame will be shown

2.1 Virtual work

When a generic structure with an applied reference load R is analyzed, the equilibrium condition can be imposed by means of the principle of virtual work. Considering an initial condition denoted with the subscript $()_0$, the principle of virtual work can be expressed as [Poulsen, 1994]:

$$\boldsymbol{\sigma}_0 \cdot \delta\boldsymbol{\varepsilon}_0 = \lambda_0 \; R \cdot \delta\mathbf{u} \tag{2.1}$$

λ_0	Initial load factor
$\boldsymbol{\sigma}_0$	Initial stress field
$\delta\boldsymbol{\varepsilon}_0$	Initial virtual strain
$\delta\mathbf{u}$	Virtual displacement

The left-hand side of Eq. (2.1) represent the internal virtual work while the righ-hand side show the external virtual work. Assuming to have an increment of the load coefficient and of the displacement field such as:

$$\begin{cases} \lambda = \lambda_0 + \Delta\lambda \\ \mathbf{u} = \mathbf{u}_0 + \Delta\mathbf{u} \\ \boldsymbol{\varepsilon} = \boldsymbol{\varepsilon}_0 + \Delta\boldsymbol{\varepsilon} \\ \boldsymbol{\sigma} = \boldsymbol{\sigma}_0 + \Delta\boldsymbol{\sigma} \end{cases} \tag{2.2}$$

The principle of virtual work for the new state can be expressed as:

$$\boldsymbol{\sigma} \cdot \delta\boldsymbol{\varepsilon} = \lambda \; R \cdot \delta\mathbf{u} \tag{2.3}$$

$\delta\boldsymbol{\varepsilon}$	Virtual strain related to $\boldsymbol{\varepsilon}$

Subtracting Eq. (2.1) to Eq. (2.3), the equation expressing the equilibrium for the incremental state is obtained; more specifically:

$$\Delta\boldsymbol{\sigma} \cdot \delta\boldsymbol{\varepsilon} + \boldsymbol{\sigma}_0 \cdot (\delta\boldsymbol{\varepsilon} - \delta\boldsymbol{\varepsilon}_0) = \Delta\lambda \; R \cdot \delta\mathbf{u} \tag{2.4}$$

In order to use the principle of virtual work to employ a buckling analysis is necessary to define all the variables involved, from load coefficient to stress fields.

2.2 Asymptotic postbuckling model

2.2.1 Strain and Stresses

As it was previously menthined in chapter 1, buckling is a non-linear phenomenon. Hence the behavior of a structure subjected to buckling cannot be fully expressed using the only linear approximation but a non-linear term has to be considered. More specifically the strain field, using the notation proposed by Byskov and Hutchinson [Poulsen and Damkilde, 1998], can be written as:

$$\boldsymbol{\varepsilon} = l_1(\mathbf{u}) + \frac{1}{2} l_2(\mathbf{u}) \tag{2.5}$$

$\boldsymbol{\varepsilon}$	Strain field
$\mathbf{u}$	Displacement field
l_1	Linear operator
l_2	Quadratic operator

The strain is describe as a sum of the standard linear strain, expressed through the linear operator l_1, and the non-linear strain expressed through the quadratic operator l_2. Using the Green-Lagrange strains with the simplification called simplified Lagrange [Rahman, 2009], Eq. (2.5) can be rewritten in an expand form as [Rahman, 2009]:

$$\begin{Bmatrix} \varepsilon_{xx} \\ \varepsilon_{yy} \\ \varepsilon_{zz} \\ \varepsilon_{xy} \\ \varepsilon_{yz} \\ \varepsilon_{xz} \end{Bmatrix} = \begin{Bmatrix} u_{x,x} \\ u_{y,y} \\ u_{z,z} \\ \frac{1}{2}(u_{x,y} + u_{y,x}) \\ \frac{1}{2}(u_{y,z} + u_{z,y}) \\ \frac{1}{2}(u_{z,x} + u_{x,z}) \end{Bmatrix} + \frac{1}{2} \begin{Bmatrix} u_{y,x}^2 + u_{z,x}^2 \\ u_{x,y}^2 + u_{z,y}^2 \\ u_{x,z}^2 + u_{y,z}^2 \\ u_{x,x}u_{x,y} + u_{y,x}u_{y,y} + u_{z,x}u_{z,y} \\ u_{x,y}u_{x,z} + u_{y,z}u_{y,y} + u_{z,z}u_{z,y} \\ u_{x,x}u_{x,z} + u_{y,z}u_{y,x} + u_{z,z}u_{z,x} \end{Bmatrix} \tag{2.6}$$

Comparing Eq.(2.5) and (2.6), it is clear how the first part of the right-hand side of Eq.(2.6) is equal to l_1 while the second part is equal to l_2. From the operators l_1 and l_2, it is also possible to define a bilinear operator by means of Eq.(2.7) [Poulsen and Damkilde, 1998]:

$$l_2(\mathbf{u} + \mathbf{v}) = l_2(\mathbf{u}) + 2 \; l_{11}(\mathbf{u},\mathbf{v}) + l_2(\mathbf{v}) \tag{2.7}$$

where $\mathbf{v}$ is an arbitrary displacement field. The bilinear operator has the following properties [Poulsen, 1994]:

$$\begin{aligned} l_{11}(\mathbf{u},\mathbf{v}) &= l_{11}(\mathbf{v},\mathbf{u}) \\ l_{11}(\mathbf{u},\mathbf{u}) &= l_2(\mathbf{u}) \end{aligned} \tag{2.8}$$

Furthermore if a virtual displacement field is applied, it is possible to derive the expression of the related virtual strain field as follow.
Considering a displacement field $\mathbf{u} + \delta\mathbf{u}$, the related strain field will be [Poulsen, 1994]:

$$\boldsymbol{\varepsilon}(\mathbf{u} + \delta\mathbf{u}) = \boldsymbol{\varepsilon}(\mathbf{u}) + \delta\boldsymbol{\varepsilon} \tag{2.9}$$

According to Eq.(2.5), the strain field can be written as:

$$\begin{aligned} \boldsymbol{\varepsilon}(\mathbf{u} + \delta\mathbf{u}) &= l_1(\mathbf{u} + \delta\mathbf{u}) + \frac{1}{2} l_2(\mathbf{u} + \delta\mathbf{u}) \\ &= l_1(\mathbf{u}) + l_1(\delta\mathbf{u}) + \frac{1}{2}[l_2(\mathbf{u}) + 2\ l_{11}(\mathbf{u},\delta\mathbf{u}) + l_2(\delta\mathbf{u})] \\ &= \left[l_1(\mathbf{u}) + \frac{1}{2} l_2(\mathbf{u})\right] + \left[l_1(\delta\mathbf{u}) + l_{11}(\mathbf{u},\delta\mathbf{u}) + \frac{1}{2} l_2(\delta\mathbf{u})\right] \end{aligned} \tag{2.10}$$

Comparing Eq. (2.5) with Eq. (2.9) and (2.10), it is possible to see how the first part of the right-hand side of Eq. (2.10) is equal to $\boldsymbol{\varepsilon}(\mathbf{u})$ while the second part correspond to $\delta\boldsymbol{\varepsilon}$. Moreover since l_2 is a quadratic operator the term $l_2(\delta\mathbf{u})$ is negligible, allowing the follow expression for the virtual strain field.

$$\delta\boldsymbol{\varepsilon} = l_1(\delta\mathbf{u}) + l_{11}(\mathbf{u},\delta\mathbf{u}) \tag{2.11}$$

Now that the strain field is fully describe the stresses, which are function of the strains, can be found using the constitutive relation [Poulsen and Damkilde, 1998]:

$$\boldsymbol{\sigma} = D(\boldsymbol{\varepsilon}) \tag{2.12}$$

If a linear elastic material is considered, it is possible to write the following reciprocity relation [Rahman, 2009]:

$$\boldsymbol{\sigma}_i \cdot \boldsymbol{\varepsilon}_j = \boldsymbol{\sigma}_j \cdot \boldsymbol{\varepsilon}_i \quad i,j = 1,2,\cdots \tag{2.13}$$

It is clear how the strain, and consequently the stresses, are function of the displacement field. Hence it is necessary to define the displacement field in all the three phases of the buckling phenomenon.

2.2.2 Koiter's asymptotic postbuckling model

To describe and predict the stability of a buckling event, Koiter suggested to express the postbuckling behavior using a perturbation series in the neighborhood of the bifurcation point. Hence the displacement field, together with the strain and stress field, can be expressed using a series in the variable ξ [Poulsen and Damkilde, 1998]. If linear prebuckling is assumed, the series can be express as[1]:

$$\mathbf{u} = \lambda \mathbf{u}_0 + \mathbf{u}_1 \xi + \mathbf{u}_2 \xi^2 + \dots \tag{2.14}$$

ξ	Mode amplitude
$\mathbf{u}_0$	Prebuckling displacement field
$\mathbf{u}_1$	Buckling mode
$\mathbf{u}_2$	Second order buckling mode

Furthermore the load coefficient can be also expressed using a pertubation series in the variable ξ, as follow:

$$\lambda = \lambda_c \, (1 + a\xi + b\xi^2 + \dots) \tag{2.15}$$

λ_c	Critical load coefficient
a	First buckling coefficient
b	Second buckling coefficient

The buckling coefficients a and b show respectively the slope and the curvature of the postbukling $\lambda - \xi$ relation at the bifourcation point as it is shown in Fig. 2.1. From the value of the two cefficients it is possible to estimate the imperfection's sensitivity of the structure, and the stability of the buckling.

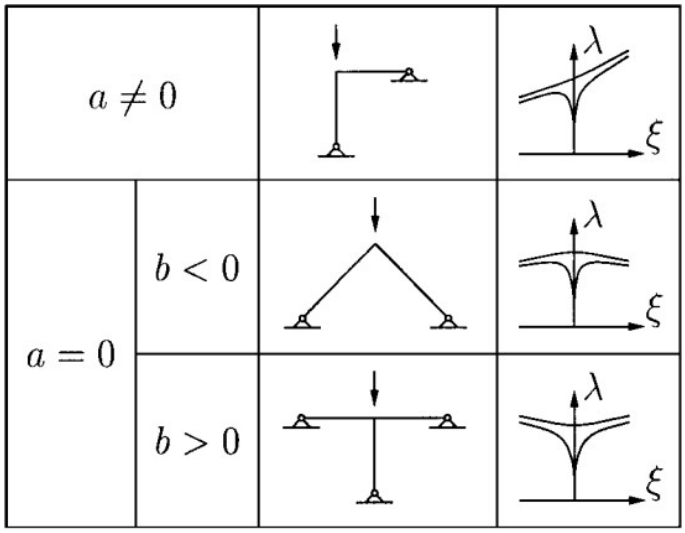

Figure 2.1. Buckling coef. and relative postbuckling behavior,[Poulsen and Damkilde, 1998]

[1]The displacement's field are chosen mutually orthogonal

The coefficient a describe the imperfection's sensitivity, while the coefficient b denote the stability of the buckling phenomenon.
Combining Eq.(2.14) and (2.15), the displacement field is expressed in terms of the buckling parameters as follow[2] [Poulsen and Damkilde, 1998]:

$$\mathbf{u} = \lambda_c \mathbf{u}_0 + (a\lambda_c \mathbf{u}_0 + \mathbf{u}_1)\xi + (b\lambda_c \mathbf{u}_0 + \mathbf{u}_2)\xi^2 + \dots \tag{2.16}$$

As Eq. (2.16) shows, the displacement field is describe like a summation that take into consideration terms of different orders and each of of them is related to a buckling phase described in chapter 1; more specifically:

- Zero-order term describe the prebuckling phase;
- First order term describe the buckling phase;
- Second and higher terms describe the postbuckling phase.

Hence it is possible to analyze a buckling phenomenon including in the analysis step by step all the different terms.

2.2.3 Virtual work and asymptotic postbuckling model

When the principle of virtual work is applied together with the asymptotic postbuckling model, it is possible to divide the problem in three sub-problem corresponding to the three buckling phases. Furthermore solving the three problem allow to calculate the three buckling parameters that are the critical load coefficient 'λ_c', the first buckling coefficient 'a' and the second buckling coefficient 'b'.

Zero-order problem

As it was previously mentioned, the zero-order problem take into consideration only the zero-order term of Eq. (2.14); i.e solving the zero-order problem is equivalent to find the solution for the prebuckling phase. The expression of the principle of virtual work for the zero-order problem is [Poulsen and Damkilde, 1998]:

$$\boldsymbol{\sigma}_0 \cdot \delta\boldsymbol{\varepsilon}_0 = \lambda_0 R \cdot \delta\mathbf{u} \tag{2.17}$$

$\boldsymbol{\sigma}_0$	Reference zero-order stress field
$\delta\boldsymbol{\varepsilon}_0$	Reference zero-order virtual strain field

According to Eq. (2.11), the zero-order virtual strain field can be expressed as:

$$\delta\boldsymbol{\varepsilon}_0 = l_1(\delta\mathbf{u}) + l_{11}(\mathbf{u}_0, \delta\mathbf{u}) \tag{2.18}$$

Since linear prebuckling is assumed, $l_{11}(\mathbf{u}_0, \delta\mathbf{u}) = 0$.
Moreover the solution of the prebuckling phase is used as a reference state, which means

[2] The same expression can be written for strain and stress field

that the load coefficient λ_0 is chosen to be equal to 1. This lead to an expression for the zero-order problem as follow.

$$\boldsymbol{\sigma}_0 \cdot l_1(\delta\mathbf{u}) = R \cdot \delta\mathbf{u} \tag{2.19}$$

First order problem

The first order problem is related to the buckling phase, i.e the structure has reached the bifurcation point. This is the point where buckling occur and consequently $\lambda = \lambda_c$. Hence the expression of the principle of virtual work related with the prebuckling phase at the bifurcation point is:

$$\boldsymbol{\sigma}_{0c} \cdot \delta\boldsymbol{\varepsilon}_{0c} = \lambda_c R \cdot \delta\mathbf{u} \tag{2.20}$$

$\boldsymbol{\sigma}_{0c}$	Critical zero-order stress field
$\delta\boldsymbol{\varepsilon}_{0c}$	Critical zero-order virtual strain field

Since linear prebuckling is assumed, the critical zero-order parameters can be found from the reference zero-order solution as:

$$\begin{cases} \mathbf{u}_{0c} = \lambda_c \ \mathbf{u}_0 \\ \boldsymbol{\varepsilon}_{0c} = \lambda_c \ \boldsymbol{\varepsilon}_0 \\ \boldsymbol{\sigma}_{0c} = \lambda_c \ \boldsymbol{\sigma}_0 \end{cases} \tag{2.21}$$

The critical solution is an equilibrium state associated with the external load $\lambda_c R$. When buckling befall the structure find an alternative state of equilibrium related with the same boundary condition of the critical solution. Furthermore the new equilibrium state can be expressed by means of the asymptotic postbuckling model. Hence including only the first order term, it is possible to express the displacement, the stress and the load coefficient as follow:

$$\begin{cases} \mathbf{u} = \lambda_c \ \mathbf{u}_0 + (a\lambda_c \mathbf{u}_0 + \mathbf{u}_1)\xi \\ \boldsymbol{\sigma} = \lambda_c \ \boldsymbol{\sigma}_0 + (a\lambda_c \boldsymbol{\sigma}_0 + \boldsymbol{\sigma}_1)\xi \\ \lambda = \lambda_c \ (1 + a\xi) \end{cases} \tag{2.22}$$

where $\boldsymbol{\sigma}_1 = D(\boldsymbol{\varepsilon}_1)$ and $\boldsymbol{\varepsilon}_1 = l_1(\mathbf{u}_1)$.
Placing the definition of the displacement field given by Eq. (2.22) into Eq. (2.11), the first order virtual strain field can be expressed as:

$$\delta\boldsymbol{\varepsilon} = l_1(\delta\mathbf{u}) + l_{11}(\mathbf{u}_1, \delta\mathbf{u})\xi \tag{2.23}$$

Analyzing Eq. (2.22), it become clear how the new equilibrium state is expressed using the first order term as an increment on the critical solution. Hence it is possible to use the expression of the principle of virtual work for an incremental state given by Eq. (2.4). Consequently the principle of virtual work for the first order problem can be expressed as:

$$(a\lambda_c \boldsymbol{\sigma}_0 + \boldsymbol{\sigma}_1)\xi \cdot \delta\boldsymbol{\varepsilon} + \lambda_c \ \boldsymbol{\sigma}_0 \cdot (\delta\boldsymbol{\varepsilon} - \delta\boldsymbol{\varepsilon}_0) = a\xi\lambda_c \ R \cdot \delta\mathbf{u} \tag{2.24}$$

Eq. (2.24) can be simplified introducing Eq. (2.18), (2.20) and (2.23). Hence the final expression become[3]:

$$\boldsymbol{\sigma}_1 \cdot l_1(\delta\mathbf{u}) + \lambda_c\ \boldsymbol{\sigma}_0 \cdot l_{11}(\mathbf{u}_1,\delta\mathbf{u}) = 0 \tag{2.25}$$

Eq. (2.25) has the form of an eigenvalue problem, whose lowest solution is the critical load factor λ_c and the associated eigenvector is the buckling mode $\mathbf{u}_1$.

Second order problem

As was previously mentioned, in order to analyze the postbuckling phase it is necessary to include into the analysis at least a second order term. Hence displacement, stress and load coefficient can be expressed as:

$$\begin{cases} \mathbf{u} = \lambda_c\ \mathbf{u}_0 + (a\lambda_c\mathbf{u}_0 + \mathbf{u}_1)\xi + (b\lambda_c\mathbf{u}_0 + \mathbf{u}_2)\xi^2 \\ \boldsymbol{\sigma} = \lambda_c\ \boldsymbol{\sigma}_0 + (a\lambda_c\boldsymbol{\sigma}_0 + \boldsymbol{\sigma}_1)\xi + (b\lambda_c\boldsymbol{\sigma}_0 + \boldsymbol{\sigma}_2)\xi^2 \\ \lambda = \lambda_c\ (1 + a\xi + b\xi^2) \end{cases} \tag{2.26}$$

Since second order effect are taken into account, the second order strain and the related stress fields, can be expressed as [Poulsen, 1994]:

$$\begin{cases} \boldsymbol{\varepsilon}_2 = l_1(\mathbf{u}_2) + \frac{1}{2}l_2(\mathbf{u}_1) \\ \boldsymbol{\sigma}_2 = D(\boldsymbol{\varepsilon}_2) = D(l_1(\mathbf{u}_2)) + D(\frac{1}{2}l_2(\mathbf{u}_1)) = \boldsymbol{\sigma}_2^{'} + \boldsymbol{\sigma}_2^{''} \end{cases} \tag{2.27}$$

With analogous considerations made for the first order problem, the second order virtual strain field can be written as:

$$\delta\boldsymbol{\varepsilon} = l_1(\delta\mathbf{u}) + l_{11}(\mathbf{u}_1,\delta\mathbf{u})\xi + l_{11}(\mathbf{u}_2,\delta\mathbf{u})\xi^2 \tag{2.28}$$

Also in this case it is possible to use the incremental state expression for the principle of virtual work since the second order term is included as an increment on the previous state. Hence the equation of the virtual work become:

$$[(a\lambda_c\boldsymbol{\sigma}_0 + \boldsymbol{\sigma}_1)\xi + (b\lambda_c\boldsymbol{\sigma}_0 + \boldsymbol{\sigma}_2)\xi^2] \cdot \delta\boldsymbol{\varepsilon} + \lambda_c\ \boldsymbol{\sigma}_0 \cdot (\delta\boldsymbol{\varepsilon} - \delta\boldsymbol{\varepsilon}_0) = (a\xi + b\xi^2)\lambda_c\ R \cdot \delta\mathbf{u} \tag{2.29}$$

Eq. (2.29) can be simplified introducing Eq. (2.18), (2.20), (2.25) and (2.28). Hence the final equation expressing the second order problem get to be[4]:

$$\boldsymbol{\sigma}_2 \cdot l_1(\delta\mathbf{u}) + \lambda_c\ \boldsymbol{\sigma}_0 \cdot l_{11}(\mathbf{u}_2,\delta\mathbf{u}) + a\lambda_c\ \boldsymbol{\sigma}_0 \cdot l_{11}(\mathbf{u}_1,\delta\mathbf{u}) + \boldsymbol{\sigma}_1 \cdot l_{11}(\mathbf{u}_1,\delta\mathbf{u}) = 0 \tag{2.30}$$

Using the definition of stress given by Eq. (2.27), Eq. (2.30) can be rewritten as:

$$\boldsymbol{\sigma}_2^{'} \cdot l_1(\delta\mathbf{u}) + \lambda_c\boldsymbol{\sigma}_0 \cdot l_{11}(\mathbf{u}_2,\delta\mathbf{u}) = -[(a\lambda_c\boldsymbol{\sigma}_0 + \boldsymbol{\sigma}_1) \cdot l_{11}(\mathbf{u}_1,\delta\mathbf{u}) + \boldsymbol{\sigma}_2^{''} \cdot l_1(\delta\mathbf{u})] \tag{2.31}$$

According to [Poulsen and Damkilde, 1998], the problem expressed by Eq. (2.31) is singular. Hence in order to find a solution an orthogonality condition is applied between $\mathbf{u}_2$ and $\mathbf{u}_1$; more specifically:

$$\boldsymbol{\sigma}_2^{'} \cdot l_1(\mathbf{u}_1) = 0 \tag{2.32}$$

[3]Since is a first order analysis all the terms allied with ξ^2 are been neglected.

[4]Since is a second order analysis all the terms allied with ξ^3 are been neglected.

Furthermore the right-hand side of Eq. (2.31) has to result orthogonal to $\mathbf{u}_1$ [Poulsen and Damkilde, 1998]. Hence replacing $\delta\mathbf{u}$ with $\mathbf{u}_1$ in the right-hand side of Eq. (2.31) and equalize it to 0, it is possible to obtain an expression for the first buckling coefficient that does not depend on the second order displacement field $\mathbf{u}_2$. The first order buckling coefficient a can be therefore expressed as:

$$a = -\frac{1}{\lambda_c}\,\frac{3}{2}\,\frac{\boldsymbol{\sigma}_1 \cdot l_2(\mathbf{u}_1)}{\boldsymbol{\sigma}_0 \cdot l_2(\mathbf{u}_1)} \tag{2.33}$$

The second order displacement field $\mathbf{u}_2$ can be now obtained by means of Eq. (2.31) together with (2.32) and (2.33).

Third order problem

Including the second order terms into the problem allow to calculate the first buckling coefficient a. To fully describe a buckling state it is necessary although to estimate also the second buckling coefficient b. Hence a third order term has to be included.
With similar consideration made for the second order problem, also the third order problem will be singular. In order to reach a solution the same orthogonality condition between $\mathbf{u}_1$ and $\mathbf{u}_2$ has to be fulfill, which lead to an expression for the b coefficient that does not depend on the third order displacement field; more specifically:

$$b = -\frac{1}{\lambda_c}\,\frac{\boldsymbol{\sigma}_2 \cdot l_2(\mathbf{u}_2) + 2\boldsymbol{\sigma}_1 \cdot l_{11}(\mathbf{u}_1,\mathbf{u}_2)}{\boldsymbol{\sigma}_0 \cdot l_2(\mathbf{u}_1)} \tag{2.34}$$

All the buckling parameters are now fully determine and is therefore possible to employ a buckling analysis using the asymptotic postbuckling model.

2.3 Example: Roodra's frame

To provide an example of results obtained by means of the asymptotic model, a Roodra's frame has been considered as it is shown below.

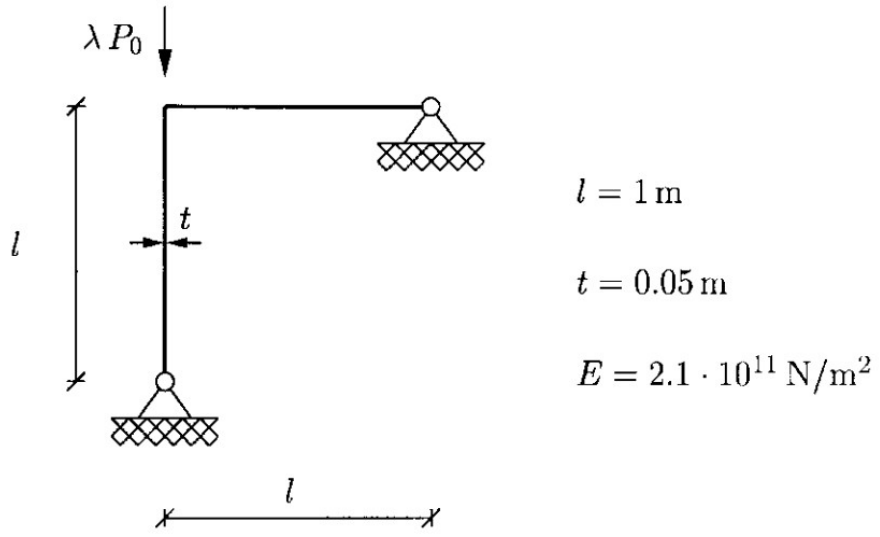

Figure 2.2. Roodra's frame,[Poulsen and Damkilde, 1998]

The two buckling parameters related to the Roodra's frame shown in Fig. 2.2 are exhibited in Tab. 2.1. All the results that are presented in the following are taken according to [Poulsen and Damkilde, 1998], since the analytical application of the asymptotic postbuckling model is out of the purpose of this work.

a	0.380520
b	0.142137

Table 2.1. Roodra's frame analytical results

The results shown above will be used further on in order to validate the results obtained by a FEM analysis.

2-D FEM Discretization 3

In this chapter it will be shown how to perform, step by step, a Finite Element Analysis in order to determine the buckling coefficients needed to express the postbuckling behavior of the structure. 2D Bernoulli beam elements and a Roodra's frame will be considered

3.1 General definition in FEM

To employ a buckling analysis with the asymptotic buckling model using FEM, it is necessary to define the linear operator l_1, the quadratic operator l_2 and the bilinear operator l_{11}. The definition of the operators in FEM is strictly related to the kind of element that is used. The following analysis is employed adopting 2D Bernoulli beam elements. Hence all the following expression are customize for the specific kind of element. A 2-D beam element with the related d.o.f*s* is depicted in Fig. 3.1.

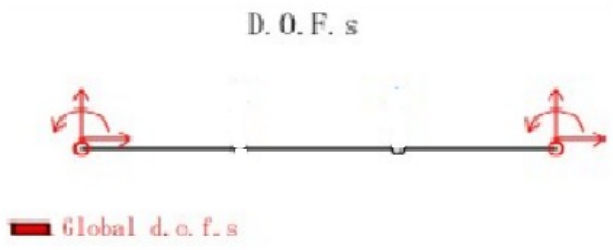

Figure 3.1. Degree of freedom for 2-D beam element

3.1.1 2-D Operators

The displacement field in FEM is interpolated using shape functions and therefore can be expressed as:

$$\mathbf{u} = \mathbf{N}\,\overline{\mathbf{V}} \tag{3.1}$$

$\mathbf{N}$	Shape function matrix
$\overline{\mathbf{V}}$	Nodal displacement vector

From Eq. (3.1), together with Eq. (2.6), it possible to derive the expression for the three operators. Since 2D beam elements are used, Eq. (2.6) will be simplified since all the strains terms out of plane are considered equal to 0.

Linear operator

The linear operator involve the first derivative of the displacement field. Hence it can be expressed by the well known strain interpolation matrix as :

$$l_1(\mathbf{u}) = \mathbf{B}\ \overline{\mathbf{V}} \tag{3.2}$$

$\mathbf{B}$ | Strain interpolation matrix

For a 2D beam element the result obtained from Eq. (3.2) is a $[2 \times 1]$ vector which contain the linear axial strain and the curvature.

Quadratic operator

Since 2D beam element are analyzed, the quadratic operator involve only the first derivative of the transverse displacement. Thus the first derivative interpolation matrix $\mathbf{G}$ can be used[1]. According to Eq. (2.6), the quadratic operator can be expressed as:

$$\begin{aligned} l_2(\mathbf{u}) &= \mathbf{I}\ \overline{\mathbf{V}}^T \mathbf{G}^T\ \mathbf{G}\overline{\mathbf{V}} \\ &= \mathbf{I}\ \overline{\mathbf{V}}^T \mathbf{S}\ \overline{\mathbf{V}} \end{aligned} \tag{3.3}$$

$\mathbf{G}$ | First derivative interpolation matrix
$\mathbf{I}$ | Auxiliary matrix

The matrix $\mathbf{G}$, for a 2D beam element with 6 dof, can be written in an expand form as:

$$\mathbf{G} = \begin{bmatrix} 0 & 0 & 0 & 0 & 0 & 0 \\ 0 & \dot{N}_i & \dot{N}_i & 0 & \dot{N}_i & \dot{N}_i \end{bmatrix} \tag{3.4}$$

$\dot{N}_i$ | First derivative of the shape fuction for the i-d.o.f

Furthermore the auxiliary matrix $\mathbf{I}$ for a 2D beam element can be expressed as:

$$\mathbf{I} = \begin{bmatrix} 1 \\ 0 \end{bmatrix} \tag{3.5}$$

The auxiliary matrix $\mathbf{I}$ assume the form expressed by Eq. (3.5) since no nonlinear effects are related to the curvature.

[1] For a beam element $\mathbf{G}$ correspond to the matrix that interpolate the rotation

Bilinear operator

As it was previously explained in chapter 2.2, the bilinear operator is defined by means of Eq. (2.7). Therefore, with some deception, the bilinear operator can be expressed as:

$$l_{11}(\mathbf{u}_a,\mathbf{u}_b) = \mathbf{I}\ \overline{\mathbf{V}}_a\ \mathbf{S}\ \overline{\mathbf{V}}_b \tag{3.6}$$

The quantities expressed by the subscript $()_a$ and $()_b$ indicate two generic displacement fields.

3.1.2 Strain and stress definitions

The application of the asymptotic postbuckling model require also the definition of strain, virtual strain and stress fields. Using the definition of the operators given above together with Eq. (2.5), (2.11) and (2.12), the expressions for the three necessary fields can be obtained.

$$\begin{aligned} \boldsymbol{\sigma} &= \mathbf{D}\boldsymbol{\varepsilon} \\ \boldsymbol{\varepsilon} &= \mathbf{B}\overline{\mathbf{V}} + \tfrac{1}{2}\mathbf{I}\ \overline{\mathbf{V}}^T\mathbf{S}\ \overline{\mathbf{V}} \\ \delta\boldsymbol{\varepsilon} &= \mathbf{B}\ \delta\overline{\mathbf{V}} + \mathbf{I}\ \overline{\mathbf{V}}\ \mathbf{S}\ \delta\overline{\mathbf{V}} \end{aligned} \tag{3.7}$$

$\mathbf{D}$	Constitutive matrix

For a 2D beam element the constitutive matrix D is written in an expand form as:

$$\mathbf{D} = \begin{bmatrix} EA & 0 \\ 0 & EI \end{bmatrix} \tag{3.8}$$

A	Cross section Area	$[m^2]$
I	Second moment of area	$[m^4]$
E	Young modulus	$[Pa]$

The result obtained from the stress relation expressed by Eq. (3.7) is a vector $[2 \times 1]$ containing the normal force and the bending moment.

3.2 FEM and the asymptotic postbuckling model

When the asymptotic postbuckling model is implemented by means of FEM, the buckling problem preserve the same structure. Thus it is possible to employ the buckling analysis following the same three phases and the related problems discussed in chapter 2; more specifically:

- Prebuckling and zero-order problem;
- Buckling and first order problem;
- Postbuckling and second or higher order problem.

The FE discretization require although some adjustmenst in order to obtain reliable results. To clearly present the procedure to follow, a Roodra's frame is taken as an example. The FEA will be carried out using Matlab and a comparison with the analytical solution presented in Table 2.1 will be done in order to validate the results.

3.2.1 Description of the structure

The Roodra's frame taken as an example, is shown in Fig 3.2.

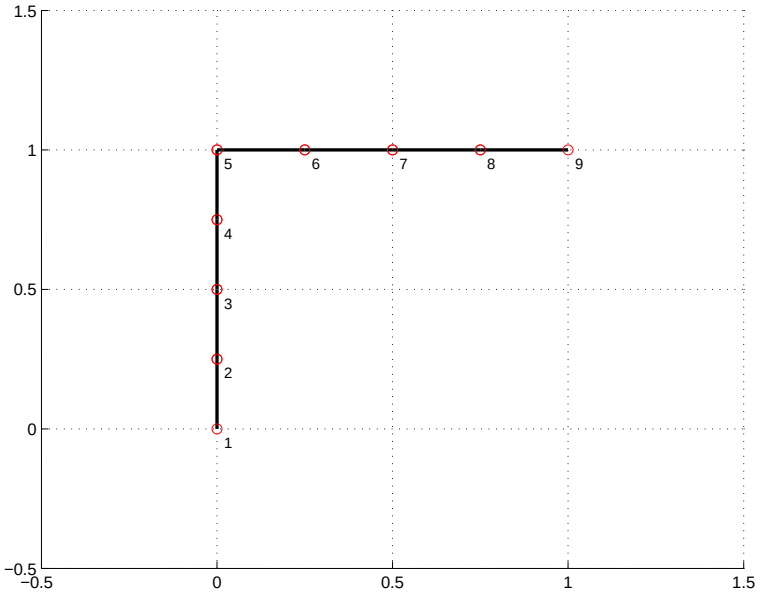

Figure 3.2. Analyzed Roodra's frame.

The structure is modeled using eight beam elements with the following specifics:

Length	L	0.25	$[m]$
Cross Section	R	0.01	$[m]$
	A	3.14×10^{-4}	$[m^2]$
	I	1.57×10^{-8}	$[m^4]$
Material	E	2.10×10^{11}	$[Pa]$
	ν	0.3	

where:

R	Radius of the cross section	$[m]$
ν	Poisson modulus	

Furthermore the analyzed frame is constrained with two pin at the free ends as shown in Fig. 3.3

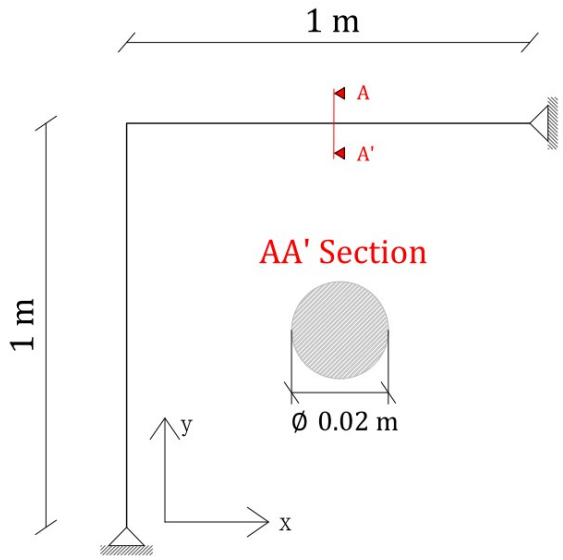

Figure 3.3. Boundary conditions Zero-order problem.

The load applied on the structure P is equal to 1 [N].
P is not the critical load, and the value is arbitrary. Nevertheless [Rahman, 2009] suggest to choose an initial value of the load not too close to the critical one otherwise the solution could be affected by an error caused by the loss of linearity when approaching the buckling point.

3.2.2 Zero-order problem

As it was previously describe in Chapter 2.2.3, the first step is to solve the zero-order problem. This is the problem in which the initial condition are applied. Thus implementing Eq.(2.19) with the operator definitions given in Chapter 3.1, the expression for the zero-order problem can be obtained[2]:

$$\mathbf{K}\ \overline{\mathbf{V}}_0 = \overline{\mathbf{F}}_0 \tag{3.9}$$

$\mathbf{K}$	Stiffness matrix
$\overline{\mathbf{V}}_0$	Zero-order nodal displacements
$\overline{\mathbf{F}}_0$	Zero-order nodal forces

Has to be noticed that Eq.(3.9) correspond to the stardard FEM equation where the stiffness matrix $\mathbf{K}$ is build from the strain interpolation matrix $\mathbf{B}$. Eq.(3.9) leads to the zero-order displacement field depicted in Fig. 3.4.

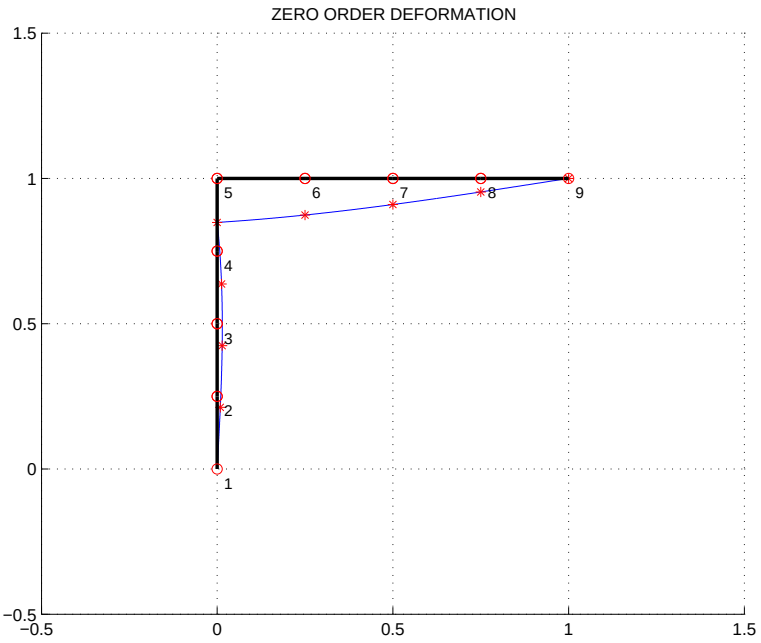

Figure 3.4. Zero-order deformation

At the displacement pictured in Fig. 3.4 is applied a scale factor of 10^7. From the displacement field $\overline{\mathbf{V}}_0$, the strain field $\boldsymbol{\varepsilon}_0$ and stress field $\boldsymbol{\sigma}_0$ can be obtained; more specifically:

$$\begin{cases} \boldsymbol{\sigma}_0 = \mathbf{D}\boldsymbol{\varepsilon}_0 \\ \boldsymbol{\varepsilon}_0 = \mathbf{B}\overline{\mathbf{V}}_0 \end{cases} \tag{3.10}$$

[2]Bernulli beam elements are considered

3.2.3 First Order Problem

The second step is to include into the analysis the first order term. The solution of the first order problem correspond to the buckling phase, i.e the bifurcation point. Finding the position of the bifurcation point means calculating the critical load factor λ_c and the related buckling mode. The critical load factor is the solution at the eigenvalue problem described by Eq. (2.25). From the definition given in Chapter 3.1, together with Eq. (2.25), it is possible to obtained the following FE expression of the eigenvalue problem:

$$(\mathbf{K} + \lambda_c \mathbf{K}_g)\,\overline{\mathbf{V}}_1 = 0; \tag{3.11}$$

$\mathbf{K}_g$	Stress Stiffness Matrix.

Using a local coordinate system denoted by ξ, it is possible to define the stress stiffness matrix for each beam element as [Poulsen and Damkilde, 1998]:

$$\mathbf{K}_g = \int_{-1}^{1} \mathbf{I}^T \boldsymbol{\sigma}_0 \; \mathbf{S} \; J d\xi \tag{3.12}$$

where J is the jacobian, and for a 2D beam element it is equal to $\frac{L}{2}$.
The stress stiffness matrix describe the change of stiffness due to the presence of a normal force in the structural element, and the matrix $\mathbf{K}_g$ for the global structure is build up as the global stiffness matrix $\mathbf{K}$.
Once the matrices are defined, it is necessary to apply the specific boundary conditions; i.e reducing the matricies $\mathbf{K}$ and $\mathbf{K}_g$. This reduction is made erasing from the two matrices columns and rows related to the known d.o.f; for the analyzed Roodra's frame it means:

$$\underbrace{\mathbf{K}}_{27\times27} \Rightarrow \underbrace{\mathbf{K}_r}_{23\times23}$$
$$\underbrace{\mathbf{K}_g}_{27\times27} \Rightarrow \underbrace{\mathbf{K}_{gr}}_{23\times23}$$

$\mathbf{K}_r$	Reduced stiffness matrix
$\mathbf{K}_{gr}$	Reduced stress stiffness matrix

Solving the eigenvalue problem expressed by Eq. (3.11) means finding the values of λ_c which fullfill the following expression:

$$det(\mathbf{K}_r + \lambda_c \mathbf{K}_{gr}) = 0 \tag{3.13}$$

The lowest value of λ_c, resulting from Eq. (3.13), is the critical load factor and the related mode is the first order buckling mode $\overline{\mathbf{V}}_1$. The value of λ_c is reported in Tab. 3.1.

λ_c	22921.17

Table 3.1. Critical load factor

Since linear prebuckling is assumed, the zero-order solution at the bifurcation point can be simply found as follow:

$$\begin{cases} \overline{\mathbf{V}}_{0cr} = \lambda_c \, \overline{\mathbf{V}}_0 \\ \overline{\mathbf{F}}_{0cr} = \lambda_c \, \overline{\mathbf{F}}_0 \\ P_{cr} = \lambda_c \, P \end{cases} \tag{3.14}$$

$\overline{\mathbf{V}}_{0cr}$	Zero order critical nodal displacement vector
$\overline{\mathbf{V}}_{0cr}$	Zero order critical nodal force vector
P_{cr}	Critical load

The first order problem is now solved and the displacement fields associated with the bifurcation point are depicted in Fig. 3.5

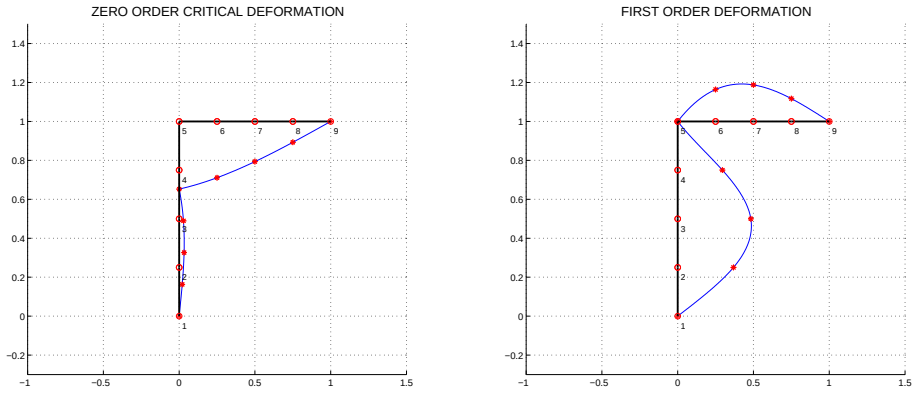

Figure 3.5. Bifurcation point displacement fields

The displacements field shown in Fig. 3.5 are scaled respectively with a factor of 10^3 and 1.
As in the zero-order problem, the first order strain and stress fileds can be estimate from the displacement field $\overline{\mathbf{V}}_1$ as follow:

$$\begin{cases} \boldsymbol{\sigma}_1 = \mathbf{D}\boldsymbol{\varepsilon}_1 \\ \boldsymbol{\varepsilon}_1 = \mathbf{B}\overline{\mathbf{V}}_1 \end{cases} \tag{3.15}$$

Eq. (3.15) will lead to an approximation of the stress state not precise enough to have a good estimation of the buckling coefficients. Hence it is necessary to apply a correction to each elements to achieve a better result.

First order local correction

When a structure deform, the load can have a secondary effect due to the deformation itself. It is possible to describe this effect with a distributed moment applied on each element as it is shown in Fig 3.6. The simple supported beam pictured in Fig 3.6 will be used as an example to better explain the procedure to apply the correction.

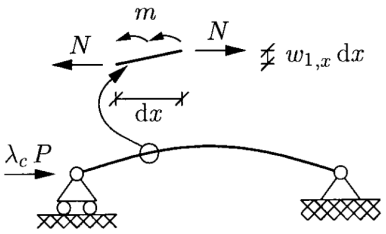

Figure 3.6. Additional distributed moment,[Poulsen and Damkilde, 1998]

As Fig. 3.6 shows, the additional moment act through the rotation and specifically through the one related with the buckling mode. Hence the distributed moment can be expressed as:

$$m(s) = N\ \theta_1(s) \tag{3.16}$$

$m(s)$	Additional distributed moment
N	Normal Force on the element.
$\theta_1(s)$	Rotation of the element related to the buckling mode.
s	Axial coordinate.

In FEM the additional load is expressed as:

$$\overline{\mathbf{M}} = -\lambda_c \mathbf{K}_g \overline{\mathbf{V}}_1 \tag{3.17}$$

$\overline{\mathbf{M}}$	Load vector related with distributed moment $m(s)$

Since for a standard beam element the transverse displacement is interpolated using a third-order polynomial, the resulting stress will have a linear variation. Referring to the simple beam depicted in Fig. 3.6, the distribution of stresses would be:

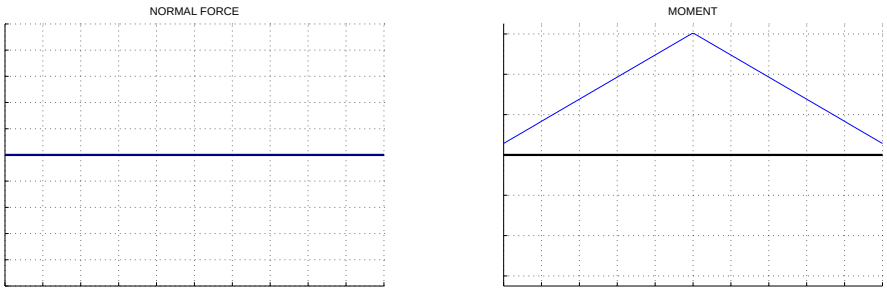

Figure 3.7. Standard distribution of stresses

According to [Poulsen and Damkilde, 1998] , to obtain a more reliable stress distribution a fifth-order polynomial variation of the transverse displacement is needed. This means adding to each element two additional nodes with a transverse d.o.f as pictured below .

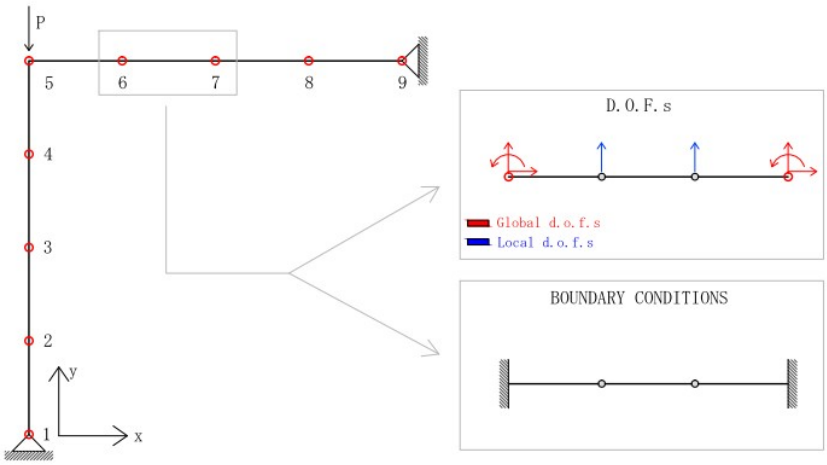

Figure 3.8. First order local correction

The local correction applied through the extra d.o.f, doesn't have to change the global solution. Thus local boundary conditions have to be applied, as pictured in Fig. 3.8. The expression for the local problem is [Poulsen and Damkilde, 1998]:

$$\mathbf{K}_l \overline{\mathbf{V}}_{1l} = -\lambda_c \mathbf{K}_{gl} \overline{\mathbf{V}}_1 \tag{3.18}$$

where:

$$\mathbf{K}_{gl} = \int_{-1}^{1} \left| \mathbf{I}^T \boldsymbol{\sigma}_0 \right| \ \mathbf{G}_l^T \mathbf{G} \ J d\xi \tag{3.19}$$

The matrix $\mathbf{G}_l$ is the local first derivative interpolation matrix and is build as the matrix $\mathbf{G}$ using the local fifth-order shape function instead. The local shape function are also use to determine the local matrix $\mathbf{B}_l$, which is used to determine the local stiffness matrix $\mathbf{K}_l$. From the local nodal displacement vector $\overline{\mathbf{V}}_{1l}$ the local stress field can be found as:

$$\begin{cases} \boldsymbol{\sigma}_{1l} = \mathbf{D}\boldsymbol{\varepsilon}_{1l} \\ \boldsymbol{\varepsilon}_{1l} = \mathbf{B}\overline{\mathbf{V}}_{1l} \end{cases} \tag{3.20}$$

Furthermore the total stress field can be found as follow and the corrected stresses are shown in Fig. 3.9.

$$\boldsymbol{\sigma}_{1tot} = \boldsymbol{\sigma}_1 + \boldsymbol{\sigma}_{1l} \tag{3.21}$$

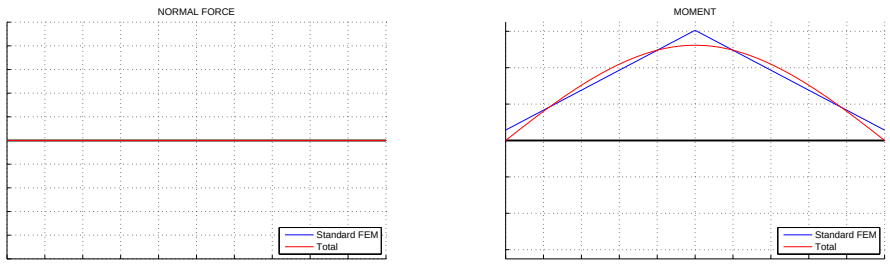

Figure 3.9. Stress with local correction applied

As depicted in Fig. 3.9, the first order correction affects only the value of the moment. This is because the load applied is a distribuited moment which will not add any contribution to the normal force. Applying the procedure explained above to each element composing the frame , the following results regarding the studied case are obtained.

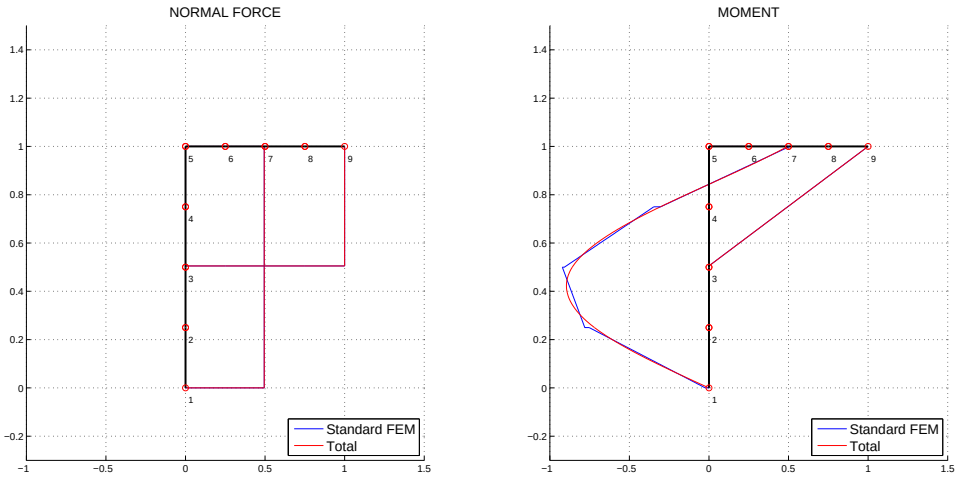

Figure 3.10. First order stresses

A scale factor of 10^{-4} is applied to both diagrams depicted in Fig. 3.10.
Once the first order stress field is obtained, it is possible to proceed with the next step.

3.2.4 Second order problem

As was previously explained in Chapter 2.2.3, the inclusion of the second order term leads to determine the first buckling coefficient a, and the second order buckling mode needed to calculate the second buckling coefficient b. The first buckling coefficient does not depend

on the second order mode, thus it is possible to compute it before solving the second order problem. By means of Eq. (2.33), together with the FEM definition of the operators previously given, it is possible to express the coefficient a as [Poulsen and Damkilde, 1998]:

$$a = -\frac{3}{2\lambda_c} \frac{\int \mathbf{I}^T \boldsymbol{\sigma}_{1tot}\ \overline{\mathbf{V}}_1^T\ \mathbf{S}\ \overline{\mathbf{V}}_1\ dV}{\int \mathbf{I}^T \boldsymbol{\sigma}_0\ \overline{\mathbf{V}}_1^T\ \mathbf{S}\ \overline{\mathbf{V}}_1\ dV} \tag{3.22}$$

The integrals in Eq. (3.22) regards the entire structure. The product $\mathbf{I}^T\boldsymbol{\sigma}_1$, which represent the normal force, is constant over the elements; i.e the expression for the a coefficient, according to [Poulsen and Damkilde, 1998], can be rewritten as:

$$a = -\frac{3}{2\lambda_c} \frac{\sum_{i=1}^{n} N_{1tot}^i\ \overline{\mathbf{V}}_{1i}^T\ \mathbf{S}_i\ \overline{\mathbf{V}}_{1i}}{\sum_{i=1}^{n} N_0^i\ \overline{\mathbf{V}}_{1i}^T\ \mathbf{S}_i\ \overline{\mathbf{V}}_{1i}} \tag{3.23}$$

n	Total number of elements
N_0^i	Zero-order normal force of the $i-$element
N_{1tot}^i	First order normal force of $i-$element
$\mathbf{S}_i$	**S**-matrix of $i-$element
$\mathbf{V}_{1i}$	First order nodal displacement vector of the $i-$element

From Eq. (3.23) the value of the first buckling coefficient is obtained and a comparison between absolute values has been done in Tab. 3.2.

Analytical	0.38052
Numerical	0.38035

Table 3.2. First buckling coefficient

The result shown in Tab. 3.2, is not sufficiently close to the analytical; i.e a bigger number of elements is needed. Once the value of the coefficient a is found, the second order problem can be solved. The FEM expression of Eq. (2.31), which represent the second order problem, is [Poulsen and Damkilde, 1998]:

$$(\mathbf{K} + \lambda_c \mathbf{K}_g)\,\overline{\mathbf{V}}_2 = -\int \left[\mathbf{S}\overline{\mathbf{V}}_1 \mathbf{I}^T (a\lambda_c \boldsymbol{\sigma}_0 + \boldsymbol{\sigma}_{1tot}) + \frac{1}{2}\mathbf{B}^T \mathbf{D}\mathbf{I}\ \overline{\mathbf{V}}_1^T \mathbf{S}\overline{\mathbf{V}}_1\right] dV \tag{3.24}$$

Eq. (3.24) can be solved as a standard FEM problem where the left hand side represent the stiffness of the structure and the right hand side the load term. However the matrix $(\mathbf{K} + \lambda_c \mathbf{K}_g)$ is singular. Hence in order to solve the problem, an extra boundary condition and an orthogonality condition between $\overline{\mathbf{V}}_1$ and $\overline{\mathbf{V}}_2$ are imposed [Poulsen and Damkilde, 1998]. The additional boundary condition is introduce adding a support at the point where the first order buckling mode vector $\overline{\mathbf{V}}_1$ has the maximum transverse displacement, as pictured in Fig. 3.11.

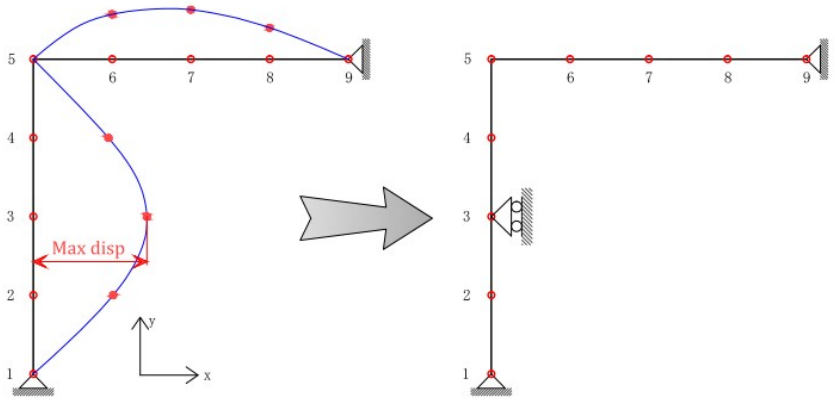

Figure 3.11. Additional boundary condition

The solution of the problem shown in Fig. 3.11, leads to a second order displacement field $\widetilde{\mathbf{V}}_2$. The displacement field represented by $\widetilde{\mathbf{V}}_2$ has to fulfill the orthogonality condition expressed by Eq. (2.32). According to [Poulsen and Damkilde, 1998], the orthogonality condition can be expressed as:

$$\overline{\mathbf{V}}_2 = \widetilde{\mathbf{V}}_2 - \frac{\overline{\mathbf{V}}_1^T \, \mathbf{K}\widetilde{\mathbf{V}}_2}{\overline{\mathbf{V}}_1^T \, \mathbf{K}\overline{\mathbf{V}}_1} \, \overline{\mathbf{V}}_1 \tag{3.25}$$

By means of Eq. (3.24) and (3.25) the displacement field depicted in Fig. 3.12 is obtained.

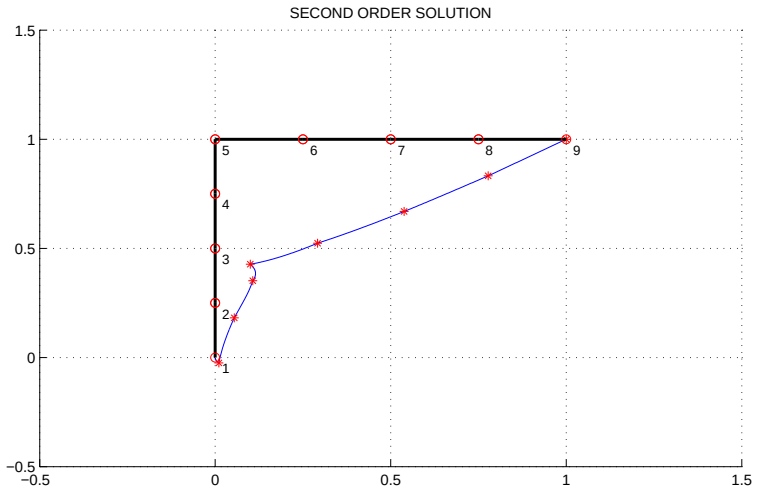

Figure 3.12. Second order deformation

The second order stress and strain field can be found from the displacement field $\overline{\mathbf{V}}_2$ as follow:

$$\begin{cases} \boldsymbol{\sigma}_2 = \mathbf{D}\boldsymbol{\varepsilon}_2 \\ \boldsymbol{\varepsilon}_2 = \mathbf{B}\overline{\mathbf{V}}_2 + \frac{1}{2}\mathbf{I}\overline{\mathbf{V}}_1^T\mathbf{S}\overline{\mathbf{V}}_1 \end{cases} \tag{3.26}$$

As it is shown by Eq. (3.26), the non linear part of the strain are included. Nevertheless also in this case it is necessary to apply a correction in order to obtain a more reliable stress field.

Second order local correction

The load applied in the second order problem, expressed by the right hand side of Eq. (3.24), is composed of two terms:

- $\overline{\mathbf{L}}_1 = \mathbf{S}\overline{\mathbf{V}}_1\mathbf{I}^T(a\lambda_c\boldsymbol{\sigma}_0 + \boldsymbol{\sigma}_{1tot})$
- $\overline{\mathbf{L}}_2 = \frac{1}{2}\mathbf{B}^T\mathbf{DI}\ \overline{\mathbf{V}}_1^T\mathbf{S}\overline{\mathbf{V}}_1$

The load vector $\overline{\mathbf{L}}_1$ is similar to the one applied in the first order problem and is therefore acting through the transverse and rotational d.o.f. On the other hand the load vector $\overline{\mathbf{L}}_2$ even though is still acting through the rotation, it is introducing a normal force in the system. According to [Poulsen and Damkilde, 1998], the correction is applied interpolating also the axial displacement with a fifth-order interpolation polynomial to have a complete fifth order displacement field. This leads to a local problem in which the elements have four additional axial d.o.f and the same local boundary condition used for the first order correction, are applied. The local problem is pictured in Fig. 3.13.

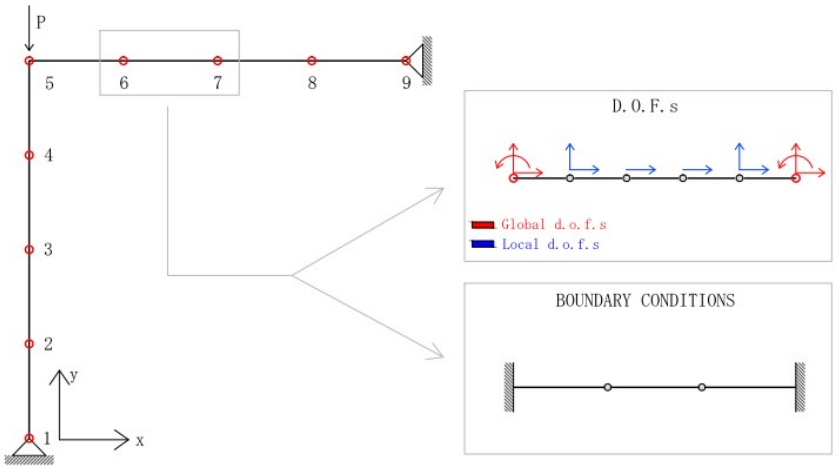

Figure 3.13. Second order correction

The second order local problem can be expressed as [Poulsen and Damkilde, 1998]:

$$\mathbf{K}_l\overline{\mathbf{V}}_{2l} = -\int [\underbrace{\mathbf{S}_l\overline{\mathbf{V}}_1\mathbf{I}^T(a\lambda_c\boldsymbol{\sigma}_0 + \boldsymbol{\sigma}_{1tot})}_{\overline{\mathbf{L}}_1} + \underbrace{\frac{1}{2}\mathbf{B}_l^T\mathbf{DI}\ \overline{\mathbf{V}}_1^T\mathbf{S}\overline{\mathbf{V}}_1}_{\overline{\mathbf{L}}_2} + \lambda_c|\mathbf{I}^T\sigma_0|\mathbf{S}_l\overline{\mathbf{V}}_2]\ dV \qquad (3.27)$$

where:

$$\mathbf{S}_l = \mathbf{G}_l\mathbf{G}$$

All the matrices with the subscript $()_l$ are related with the local element and are build as the standard matrices using the fifth-order shape functions instead. Form the local displacement vector $\overline{\mathbf{V}}_{2l}$, the local second order strain and stress field are obtained as:

$$\begin{cases} \boldsymbol{\sigma}_{2l} = \mathbf{D}\boldsymbol{\varepsilon}_{2l} \\ \boldsymbol{\varepsilon}_{2l} = \mathbf{B}_l\overline{\mathbf{V}}_{2l} \end{cases} \tag{3.28}$$

The local problem is solved following a standard linear analysis and therefore the non-linear strain doesn't play any role in the determination of the strain and stress field. As for the first order problem, the total stress field can be found as:

$$\boldsymbol{\sigma}_{2tot} = \boldsymbol{\sigma}_2 + \boldsymbol{\sigma}_{2l} \tag{3.29}$$

The solution to Eq. (3.29) is depicted in Fig. 3.14.

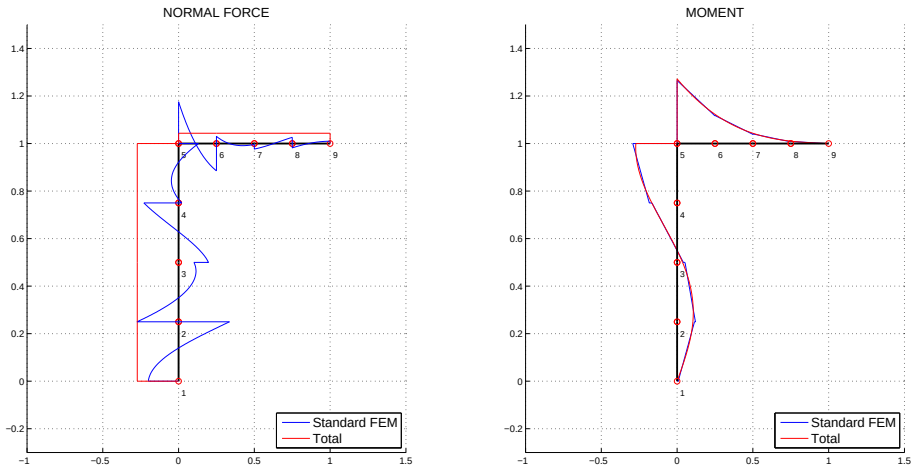

Figure 3.14. Second order stresses

3.2.5 Third order problem

In order to estimate the second buckling coefficient b it is necessary to include a third order term from the asymptotic postbuckling model. As was previously mentioned, when the orthogonality condition between the first and the second order displacement field is applied to the third order problem, Eq. (2.34) is found. According to [Poulsen and Damkilde, 1998], Eq. (2.34) can be rewritten, in a FEM environment, as:

$$b = -\frac{1}{\lambda_c}\frac{\int[\mathbf{I}^T\boldsymbol{\sigma}_{2tot}\ \overline{\mathbf{V}}_1^T\ \mathbf{S}\ \overline{\mathbf{V}}_1 + 2\mathbf{I}^T\boldsymbol{\sigma}_{1tot}\ \overline{\mathbf{V}}_2^T\ \mathbf{S}\ \overline{\mathbf{V}}_1]\ dV}{\int \mathbf{I}^T\boldsymbol{\sigma}_0\ \overline{\mathbf{V}}_1^T\ \mathbf{S}\ \overline{\mathbf{V}}_1\ dV} \tag{3.30}$$

As pictured in Fig. 3.14, the second order corrected normal force is constant over the element. Therefore, as for the first buckling coefficient, Eq. (3.30) can be written as:

$$b = -\frac{1}{\lambda_c} \frac{\sum_{i=1}^{n} N_{2tot}^{i}\ \overline{\mathbf{V}}_{1i}^{T}\ \mathbf{S}_i\ \overline{\mathbf{V}}_{1i} + 2N_{1tot}^{i}\ \overline{\mathbf{V}}_{2i}^{T}\ \mathbf{S}_i\ \overline{\mathbf{V}}_{1i}}{\sum_{i=1}^{n} N_{0}^{i}\ \overline{\mathbf{V}}_{1i}^{T}\ \mathbf{S}_i\ \overline{\mathbf{V}}_{1i}} \tag{3.31}$$

N_{2tot}^{i}	Second order normal force of $i-$element
$\mathbf{V}_{2i}$	Second order nodal displacement vector of the $i-$element

The second order buckling coefficient b is calculated by means of Eq. (3.31). A comparison with the analytical solution has been made in Tab. 3.3.

Analytical	0.142137
Numerical	0.142016

Table 3.3. Second order buckling coefficient

As for first buckling coefficient, it is necessary to use a higher number of elements to obtain a more reliable result. Since the values of the load factor λ_c and of the two buckling coefficients a and b depend on the number of elements used to model the frame, a convergence analysis has been employed to obtained the necessary number of elements to reach acceptable results. The convergence analysis has been carried out using the following number of elements.

$$n_{elem} = \begin{bmatrix} 8 & 10 & 16 & 20 & 32 & 40 & 50 & 64 \end{bmatrix}$$

The outcomes of the convergence analysis are depicted in Fig 3.15.

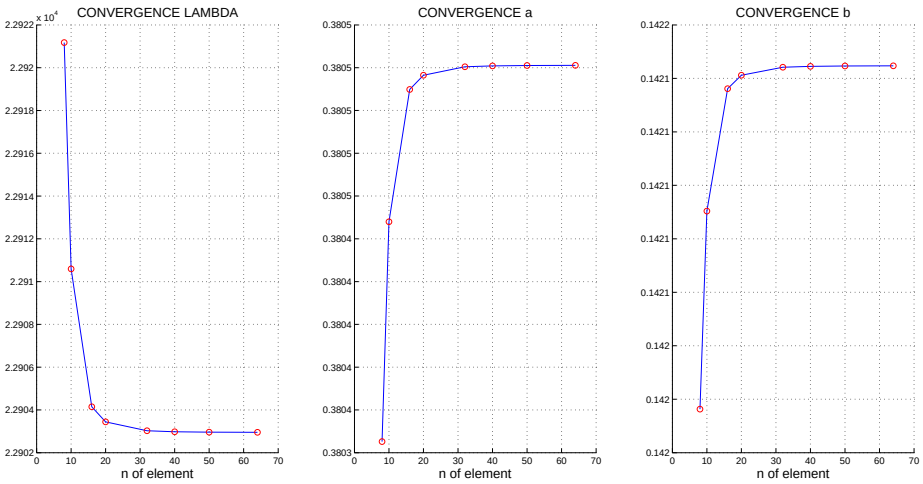

Figure 3.15. Convergence analysis

As Fig. 3.15 shows, the three buckling parameters reach convergence when a total number of 32 element is used and the values of the parameters are shown below.

	Analytical	Numerical
a	0.380520	0.380520
b	0.142137	0.142144

Table 3.4. Converged buckling parameters

Once the values of the three buckling parameters are found, the function describing the variation of the load coefficient respect to the displacement can be found as follow.

$$\lambda(\mathbf{u}) = \frac{\mathbf{u} - \mathbf{u}_1\xi - \mathbf{u}_2\xi}{\mathbf{u}_0} \tag{3.32}$$

The variable ξ represent the mode amplitude which value can be found by means of Eq. (2.15), changing the load factor [Rahman, 2009]. Furthermore for $\lambda \leq \lambda_c$, the mode amplitude ξ is equal to 0 and λ has a linear variation with a slope equal to $\frac{1}{\mathbf{u}_0}$.

3.3 ABAQUS non-linear analysis: 2-D

A non-linear analysis using ABAQUS is performed in order to confirm the accuracy of the asymptotic postbuckling model. The accuracy is validated comparing the $\lambda - u$ relation obtained from ABAQUS and from the FEM code developed in the previous chapter. The ABAQUS model is made using 2-D beam elements with the same geometrical and material characteristics as the model shown in Chapter 3.2.1. In order to obtain the $\lambda - u$ relation, two analysis are employed:

- Buckling analysis
- Non-linear analysis

Buckling analysis

The buckling analysis is performed in order to obtained the critical load to apply in order to highlight the postbuckling behavior in the further non-linear analysis. The same static and kinematic boundary conditions described in Chapter 3.2.1 are used; i.e a load equal to -1$[N]$ at the corner and two pin at the free ends of the frame are imposed as pictured in Fig. 3.17. Furthermore 32 elements are used to model the frame in order to be consistent with the previous analysis.

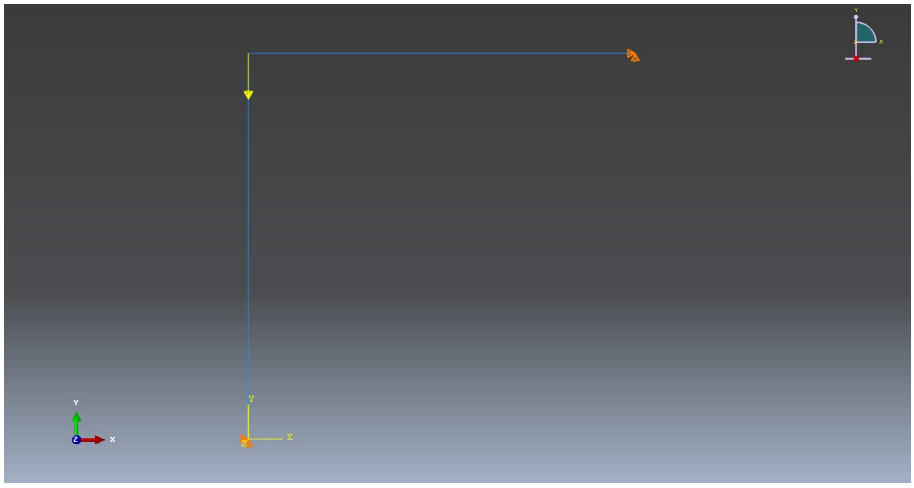

Figure 3.16. ABAQUS roodra's frame model

The buckling analysis give the following buckling mode and critical load factor.

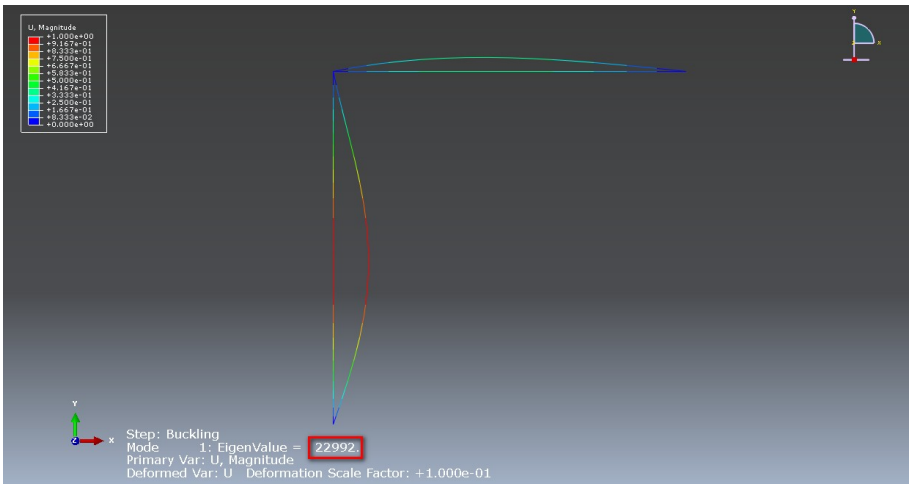

Figure 3.17. ABAQUS buckling mode

	Matlab	ABAQUS
λ_c	22903	22992

Table 3.5. Critical load factors

The difference between the results displayed in Tab. 3.5 is of the 0.004%. Such a small difference was expected since the eigenvalue problem is the same for both solver. Furthermore the critical load factors correspond,in absolute value, to the critical load since the initial load applied has an absolute value equal to 1 $[N]$.

Non-linear analysis

The non-linear analysis follow the buckling analysis and is performed in order to obtain the $\lambda - u$ relation. While the kinematic boundary condition are the same applied in the buckling analysis, some considerations are needed regarding the static boundary condition. Hence to ensure a good approximation of the postbuckling behavior, the load is applied with the following specifics:

- Same location as for the buckling analysis;
- A bigger value then the critical load; more specifically the load has been chosen equal to -25000 $[N]$.
- A small value of load step; in particular it is imposed equal to 0.001.

Due to the high non-linearity close to bifurcation point, the non-linear analysis fail and the result corresponding to the last load step is depicted below.

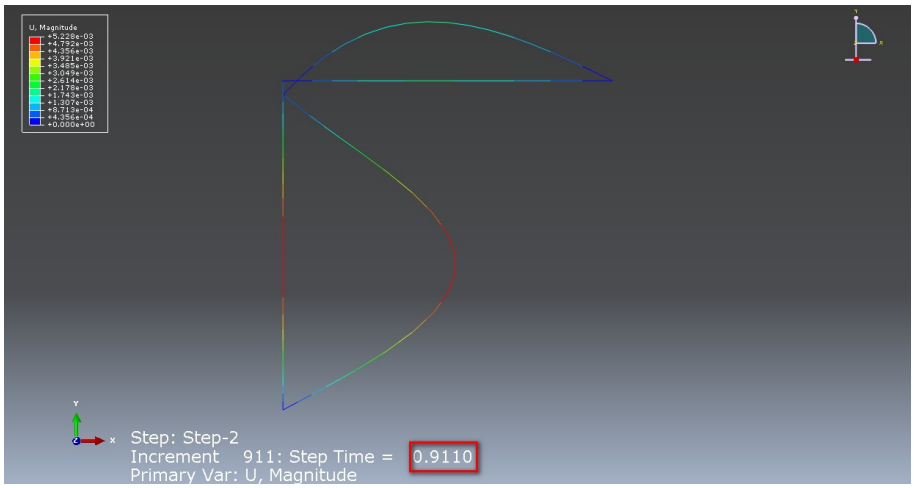

Figure 3.18. ABAQUS Non-linear deformation

ABAQUS allow to pull out the value of the displacement of one of the node for each load increment. Hence to build the $\lambda - u$ relation, the transverse displacement of node number 9 has been chosen for both ABAQUS and Matlab model as indicated in Fig. 3.19

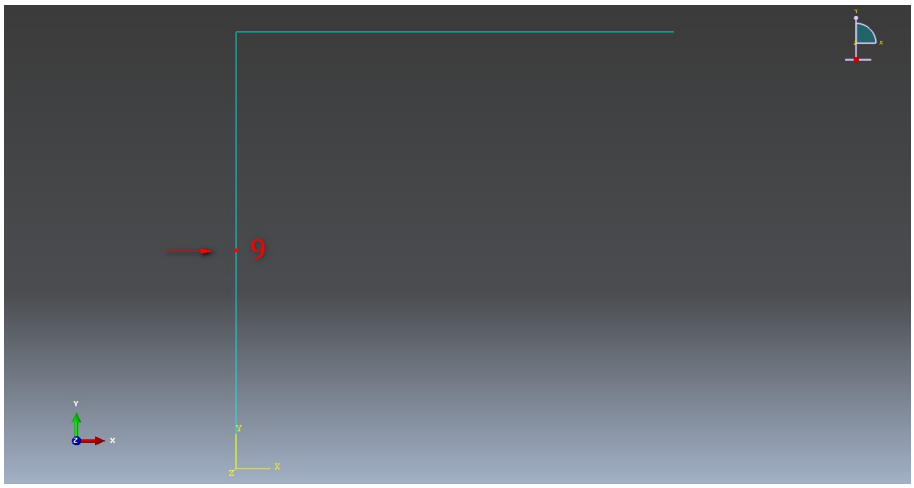

Figure 3.19. Node for $\lambda - u$ relation

The results from both non-linear analysis and asymptotic postbuckling model are picture in Fig. 3.20.

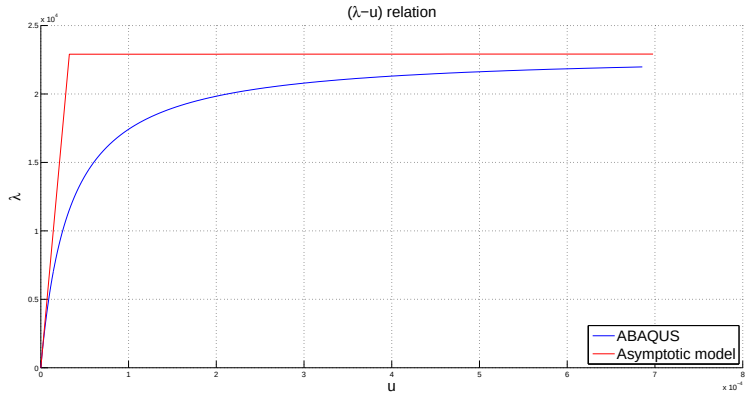

Figure 3.20. Load factor-displacement relation

To better evaluate the variation of the asymptotic postbuckling model, a zoom at the neighborhood of the bifurcation point is pictured in Fig. 3.20. Analyzing the depicted results, the following conclusion can be done:

1. The results obtained from the ABAQUS non-linear analysis suggest a strong imperfection sensitivity due to the fact that, a loss of linearity is already evident for a load equal to the 40% of the critical load. This is confirmed by the asymptotic model results, which present a value of the a-coefficient bigger than 0. To achieve a more reliable $\lambda - u$ relation with the asymptotic postbuckling model, non-linear prebuckling should be considered.

2. Comparing the Fig. 3.20 with 1.2, it can be seen how the obtained results satisfy the expectation regarding the postbuckling behavior of the Roodra's frame. As a further confirmation, a zoom of the asymptotic model at the neighborhood of the bifurcation point is plotted below.

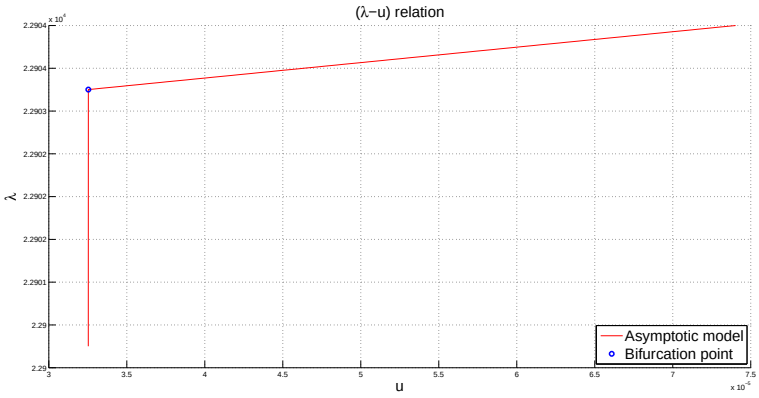

Figure 3.21. Asymptotic postbuckling relation

Fig. 3.21 show a significant change in slope at the bifurcation point, slope that remain positive for value of λ bigger then the critical one.

3-D Buckling analysis 4

In this chapter the buckling phenomenon in a three dimensional space will be briefly analyzed. The impact of the torsion will be considered, focusing on the torsional buckling modes and the warping effect. Furthermore strains and stresses fields will be defined following the Bernoulli beam theory and the governing equations of the asymptotic postbuckling model for a 3-D case will be given.

4.1 3-D Buckling and thin walled beam

4.1.1 Torsional buckling modes

When the buckling phenomenon is analyzed in a 3-D space, the Euler buckling mode is not the only mode that can appear and the buckling strength can result in a lower value then the one considered in a two dimensional case. The additional mode are related with the torsion of the cross section and are named:

- Flexural-torsional buckling
- Lateral-torsional buckling

The flexural-torsional buckling is a consequence of a compression on a structural element as shown below.

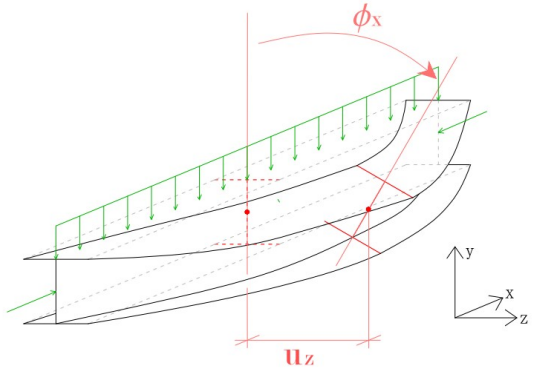

Figure 4.1. Flexural-buckling mode

The flexural-buckling mode occur when the section of the beam has a low value of torsional stiffness (e.g open cross section) and a low value of bending stiffness at least around one of the axis. Due to the compressive load, the beam can buckle with a resulting deviation of the beam axis. If a vertical load is applied as shown in Fig. 4.1, the deviation can add an eccentricity to the load which can introduce a torque with a resulting twist of the cross section. The flexural-torsional mode will therefore be a mix of bending and twisting.
On the other hand, the lateral-torsional buckling mode is exhibit in a more local scale in which local elements of the cross section are involved; e.g. the flanges of I-profile.

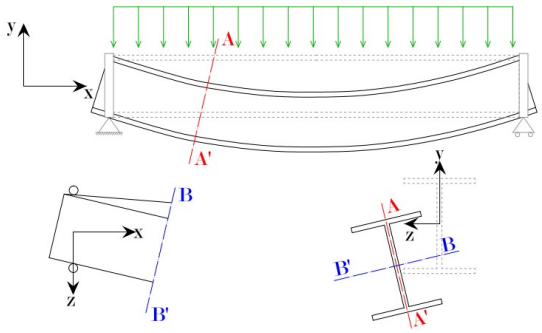

Figure 4.2. Lateral-buckling mode [Carlos Luis Badillo Bercebal, 2014]

Furthermore the just mentioned mode occur when the beam is subjected to flexural loads that cause compression of one of the element of the cross section like shown in Fig. 4.2. In the pictured case, the upper flange is subjected to compressive stresses introduced by the bending moment. The flange is the point on the cross sectional plane were the biggest value of stress is found. Hence the compressive stresses can reach the critical value for which the flange can buckle laterally in its plane. Hence the deflection can add eccentricity to load, bringing out some torsion causing twisting of the section. As for the flexural-torsional buckling mode, the lateral-torsional buckling mode occur for section with a small torsional resistance, such as I-profiles.

4.1.2 Torsion on thin-walled beams

When a torque is applied on an open cross section, e.g. I-profile, it can cause some secondary effect; i.e warping. Warping is a deformation out of the plane of the cross section due to torsion, as shown in Fig. 4.3, and usually occur on the so-called thin-walled beams.

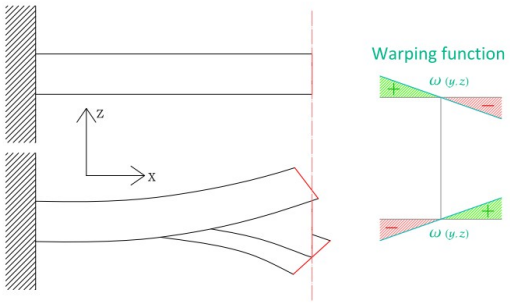

Figure 4.3. Warping

A beam is defined as thin-walled when:

$$\begin{cases} \dfrac{b}{L} < 0.1 \\ \dfrac{t}{b} < 0.1 \end{cases} \tag{4.1}$$

b	Typical cross section dimension
t	Thickness
L	Length of the beam

If the warping deformation is constrained, it will introduced in the system some additional normal stresses on some of the cross section elements, e.g. the flanges of an I-profile. The variation of the warping normal stresses over the cross sectional plane is defined by the warping functions. For each cross section is possible to find the related warping function but this is out of the purpose of this work. For an I-profile the warping function are pictured in Fig. 4.3. Warping is an important phenomenon to take into consideration,especially for the lateral-torsional buckling mode, since is introducing normal stresses on a local scale that can affect the buckling strength of the structure.

4.2 Strain and stress definition

In a static structural analysis, it is possible to take into account the effects of the two buckling modes and of warping by redefining the strain and consequently the stress field. Since Bernoulli beam theory is considered, a particular attention will be put in the definition of the normal strain. Hence the normal strain field can be defined as:

$$\varepsilon_{xx} = \varepsilon_{xx}^{lin} + \varepsilon_{xx}^{n-lin} \tag{4.2}$$

ε_{xx}^{lin}	Linear strain
ε_{xx}^{n-lin}	Non-linear strain

The difference from the 2-D case is that both ε_{xx}^{lin} and ε_{xx}^{n-lin} are not constant over the cross sectional plane. According to [Jesper Dencker Larsen, 2007] the kinematic of a 3-D beam can be expressed as below. The subscript $()_{,x}$ indicate the derivative by x and the expressions make reference to the coordinate system shown in Fig. 4.1 :

$$\begin{cases} u_x(x,y,z) = u_x(x) - y\ u_{y,x} - z\ u_{y,x} - \omega(y,z)\phi_{,x}(x) \\ u_y(x,y,z) = u_y(x) - z\ \phi(x) \\ u_z(x,y,z) = u_z(x) + y\ \phi(x) \end{cases} \tag{4.3}$$

$\omega(y,z)$	Warping function
$\phi(x)$	Twisting angle function

From Eq. (4.3) it is possible to see how the torsion has been included in the kinematic by means of twisting angle ϕ and its derivative. From the Green strain definition given by Eq. (2.6), inserting Eq. (4.3), it is possible to reach with some deceptions the following expression for the axial strain[Jesper Dencker Larsen, 2007]:

$$\begin{aligned} \varepsilon_{xx} =& u_{x,x}(x) - \omega(y,z)\phi_{,xx}(x) + \frac{1}{2}u_{y,x}^2(x) + \frac{1}{2}u_{z,x}^2(x) + \frac{1}{2}\phi_{,x}^2(x)\ (z^2+y^2) - \\ & - u_{y,x}(x)\phi_{,x}(x)\ z + u_{z,x}(x)\phi_{,x}(x)\ y \end{aligned} \tag{4.4}$$

From Eq. (4.4) the different terms related with different effect can be isolated.

4.2.1 Linear strain

The linear part of the strain is represented by the first two terms of Eq. (4.4); more specifically:

$$\varepsilon_{xx}^{lin} = u_{x,x}(x) - \omega(y,z)\phi_{,xx}(x) \tag{4.5}$$

As it can be seen from Eq. (4.5), warping has been included by means of the warping function $\omega(y,z)$. For a double symmetric cross section such as the I-profile, the elastic center coincide with the shear center; i.e. the warping function is equal to 0 at the elastic center[1].

[1] The elastic center also coincide with the origo of the beam coordinate system

4.2.2 Non-Linear strain

The non-linear strain is expressed by the remaining five terms of Eq. (4.4). They can be placed in three different groups, each one of those represent a specific non-linear effect; more specifically:

• Euler buckling	$\Rightarrow$	$\frac{1}{2}u_{y,x}^2(x) + \frac{1}{2}u_{z,x}^2(x)$
• Fexural-torsional buckling	$\Rightarrow$	$\frac{1}{2}\phi_{,x}^2(x)\ (z^2 + y^2)$
• Lateral-torsional buckling	$\Rightarrow$	$-u_{y,x}(x)\phi_{,x}(x)\ z + u_{z,x}(x)\phi_{,x}(x)\ y$

Table 4.1. Non-linear effect

The non-linear strain, which is a summation of the three non-linear strain group presented above, is the one defining the buckling mode of the structure.

Shear strain

Even though the following analysis is carried out using Bernoulli beam theory, it is still important to define the shear strain since, in a three dimensional case, they play a role in the determination of the bifurcation point. Hence, according to [Jesper Dencker Larsen, 2007], the shear strains can be expressed as:

$$\begin{aligned} \gamma_{xy} &= u_{z,x}(x)\ \phi(x) \\ \gamma_{xz} &= -u_{y,x}(x)\ \phi(x) \end{aligned} \tag{4.6}$$

γ_{xy}, γ_{zy}	Non-linear shear strain

The expression given by Eq. (4.6) show only the non-linear part of the shear strains since are the only one of interest when Bernoulli beam theory is used together with the asymptotic postbuckling model.
Once the strain field is define, the stress field can be obtained using the constitutive relation:

$$\boldsymbol{\sigma} = D(\boldsymbol{\varepsilon}) \tag{4.7}$$

The constitutive relation in a 3-D case will be obviously different from the 2-D case due to the torsional effects. A more detailed expression will be given later in the FEM implementation.

4.3 Virtual work and asymptotic postbuckling model: 3-D case

When the asymptotic postbuckling model is applied in a 3-D case, the same operational definition of the strain, given by Eq. (2.5), can be used since the difference between the 2-D and 3-D case subsist in the displacement field definition. Hence the description of the

buckling behavior in a three dimensional space can be done following the same procedure describe in Chapter 2.2.3 ; i.e. dividing the problem in four sub-cases, in which an higher term of the postbuckling model will be included step-by-step in order to find the three buckling coefficients defining the buckling behavior of the structure. Nevertheless a recall of the four problems and related equations are shown below.

- Zero-order problem $\Rightarrow \quad \boldsymbol{\sigma}_0 \cdot l_1(\delta\mathbf{u}) = R \cdot \delta\mathbf{u}$
- First order problem $\Rightarrow \quad \boldsymbol{\sigma}_1 \cdot l_1(\delta\mathbf{u}) + \lambda_c \, \boldsymbol{\sigma}_0 \cdot l_{11}(\mathbf{u}_1,\delta\mathbf{u}) = 0$
- Second order problem $\Rightarrow$
$$\begin{cases} \boldsymbol{\sigma}_2^{'} \cdot l_1(\delta\mathbf{u}) + \lambda_c \boldsymbol{\sigma}_0 \cdot l_{11}(\mathbf{u}_2,\delta\mathbf{u}) = \\ = -[(a\lambda_c\boldsymbol{\sigma}_0 + \boldsymbol{\sigma}_1) \cdot l_{11}(\mathbf{u}_1,\delta\mathbf{u}) + \boldsymbol{\sigma}_2^{''} \cdot l_1(\delta\mathbf{u})] \\ a = -\dfrac{1}{\lambda_c} \, \dfrac{3}{2} \, \dfrac{\boldsymbol{\sigma}_1 \cdot l_2(\mathbf{u}_1)}{\boldsymbol{\sigma}_0 \cdot l_2(\mathbf{u}_1)} \end{cases}$$
- Third order problem $\Rightarrow \quad b = -\dfrac{1}{\lambda_c} \, \dfrac{\boldsymbol{\sigma}_2 \cdot l_2(\mathbf{u}_2) + 2\boldsymbol{\sigma}_1 \cdot l_{11}(\mathbf{u}_1,\mathbf{u}_2)}{\boldsymbol{\sigma}_0 \cdot l_2(\mathbf{u}_1)}$

The operational notation can still be used, but some adjustments will be done in the FEM formulation due to the fact that shear's effects are not directly considered.

3-D FEM Discretization 5

In this chapter a 3-D FE implementation of the asymptotic postbuckling model will be employed. The FE implementation of the asymptotic model will be shown recalling the theory explained in Chapter 2. The discussion will be expanded to a 3-D case where thin walled beam stresses effects will be included. A 3-D Bernoulli beam model will be used and the same steps made for the 2-D discretization will be followed. All the discussion will be supported by a step-by-step application of the model to a simple steel frame structure

5.1 General FEM definitions

In the following will be presented the implementation of the asymptotic postbuckling model using 3-D beam element. Three dimensional beam element used by commercial programs such as ABAQUS, have 6 d.o.f per node which correspond to three translation e three rotation. In order to take into account warping, an extra d.o.f is needed as shown below.

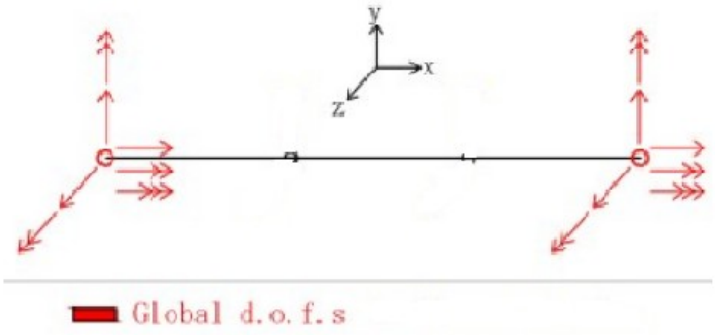

Figure 5.1. Degree of freedom for 3-D beam element

The extra d.o.f, $\phi_{,x}$, correspond to the derivative of the twisting angle and is treated in the same manner as the transverse displacements and relative rotation where the latter is the derivative of the former. Therefore at each d.o.f is assigned a shape function, used to define the 3-D displacement field and the operators. The expression of the shape functions of each d.o.f can be found in Appendix B. Furthermore the coordinate system of the beam element is located at the elastic center where the warping function as a

value equal to 0 and therefore has any impact on the definition of the linear strain field[1]. Furthermore it is important to mention that even though Bernoulli beam theory is used in the FEM implementation, shear stresses play an important role in the buckling analysis and therefore it will be necessary to define separately all the static quantities related to the shear.

5.1.1 3-D Operators

As for the two dimensional case, three operators have to be defined; more specifically:

- Linear operator
- Quadratic operator
- Bilinear operator

All the operators are defined in the beam local coordinate system pictured in Fig. 5.1.

Linear operator

The linear operator define the linear strain, and therefore can be expressed as:

$$l_1(\mathbf{u}) = \mathbf{B}\ \overline{\mathbf{V}} \tag{5.1}$$

Linear shear strains are not considered since Bernoulli beam theory has been used to model the beam elements.

Quadratic operator

The second to be defined is the quadratic operator that define the non-linear part of the strain. The non-linear strains that play a role in the employed analysis are the axial and the shear strains. Even though the shear strains are not directly included in the FE formulation, it is possible to take them into consideration defining them separately as will be shown in the following. A general expression for a quadratic operator is:

$$l_2(\mathbf{u}) = \mathbf{I}\ \overline{\mathbf{V}}^T \mathbf{S}\ \overline{\mathbf{V}} \tag{5.2}$$

For a better understanding of the three different non-linear effects, the quadratic operator is divided as follow:

$$l_2(\mathbf{u}) = l_{2,eu}(\mathbf{u}) + l_{2,ft}(\mathbf{u}) + l_{2,lt}(\mathbf{u}) \tag{5.3}$$

$l_{2,eu}(\mathbf{u})$	Quadratic operator for euler effect
$l_{2,ft}(\mathbf{u})$	Quadratic operator for flexural-torsional effect
$l_{2,lt}(\mathbf{u})$	Quadratic operator for lateral-torsional effect

To each one of the quadratic operator is associated a specific auxiliary matrix $\mathbf{I}$ and a matrix $\mathbf{S}$. Hence all the operators are define as follow.

[1]Some of the expression in the following will be the same as for the 2-D case but the dimension of the involved vectors and matrices will be different.

1. **Euler buckling effect**. It is describe by the two bending rotation and can be express as:

$$l_{2,eu}(\mathbf{u}) = \mathbf{I}_{eu}\ \overline{\mathbf{V}}^T \mathbf{S}_{eu}\ \overline{\mathbf{V}} \tag{5.4}$$

The Euler buckling effect introduce a non-linearity in the normal strain and is strictly related to the normal stresses. Therefore the matrix $\mathbf{I}_{eu}$ can be written in an expand form as:

$$\mathbf{I}_{eu} = \begin{bmatrix} 1 \\ 0 \\ 0 \\ 0 \\ 0 \end{bmatrix}$$

Furthermore the matrix $\mathbf{S}_{eu}$ is build using the bending rotation interpolation matrix and, recalling the equation shown in Tab. 4.1, can be expressed as:

$$\mathbf{S}_{eu} = \mathbf{G}_z^T\ \mathbf{G}_z + \mathbf{G}_y^T\ \mathbf{G}_y \tag{5.5}$$

$\mathbf{G}_y$	Interpolation matrix for rotation around y-axis
$\mathbf{G}_z$	Interpolation matrix for rotation around z-axis

2. **Flexural-torsional effect**. As the Euler buckling effect, the flexural-torsional effect is also connected to the normal force. Hence the quadratic operator can be written using the following expression:

$$\begin{cases} l_{2,ft}(\mathbf{u}) = \mathbf{I}_{ft}\ \overline{\mathbf{V}}^T \mathbf{S}_{ft}\ \overline{\mathbf{V}} \\ \mathbf{I}_{ft} = \mathbf{I}_{eu} \end{cases} \tag{5.6}$$

The flexural-torsional effect is related to the twisting angle as shown in Tab. 4.1. Therefore the matrix $\mathbf{S}_{ft}$ can be expressed as:

$$\mathbf{S}_{ft} = (z^2 + y^2) \cdot \mathbf{G}_\phi^T\ \mathbf{G}_\phi \tag{5.7}$$

$\mathbf{G}_\phi$	Interpolation matrix for twisting angle
z, y	Coordinate on the cross sectional plane

As it can be seen the matrix $\mathbf{S}_{ft}$ is a function of z and y, which indicate a variation on the cross sectional plane. Hence evaluating the flexural-torsional operator at the elastic center will result in a value equal to 0.

3. **Lateral-torsional effect**. Differently from the previous two operators, the quadratic operator related to the lateral-torsional effect is directly connected to the applied bending moment and the shear force. The non-linearity introduced by the lateral-torsional phenomenon can be therefore considered linked to the curvature, according to [Jesper Dencker Larsen, 2007], and shear strain. Due to the fact that shear's effects are not directly considered into the analysis, it will be necessary to

define a non-linear operator specifically for the non-linear shear strain. Hence the quadratic operators for the lateral-torsional effect can be expressed as follow. For a better understanding the terms related with the local y and z axis are considered separately.

$$l_{2,lt}(\mathbf{u}) \Rightarrow \begin{cases} l^c_{2,lt}(\mathbf{u}) = \mathbf{I}^y_{lt}\ \overline{\mathbf{V}}^T \mathbf{S}^y_{ft}\ \overline{\mathbf{V}} + \mathbf{I}^z_{lt}\ \overline{\mathbf{V}}^T \mathbf{S}^z_{ft}\ \overline{\mathbf{V}} \\ l^s_{2,lt}(\mathbf{u}) = \mathbf{I}^y_{sh}\ \overline{\mathbf{V}}^T \mathbf{S}^y_{sh}\ \overline{\mathbf{V}} + \mathbf{I}^z_{sh}\ \overline{\mathbf{V}}^T \mathbf{S}^z_{sh}\ \overline{\mathbf{V}} \end{cases} \tag{5.8}$$

$l^c_{2,lt}(\mathbf{u})$	Quadratic operator for lateral-torsional effect (Curvature)
$l^s_{2,lt}(\mathbf{u})$	Quadratic operator for lateral-torsional effect (Shear)

The four auxiliary matrices can be written in an expand form as:

$$\mathbf{I}^y_{lt} = \begin{bmatrix} 0 \\ 1 \\ 0 \\ 0 \\ 0 \end{bmatrix}; \quad \mathbf{I}^z_{lt} = \begin{bmatrix} 0 \\ 0 \\ 1 \\ 0 \\ 0 \end{bmatrix}; \quad \mathbf{I}^y_{sh} = \begin{bmatrix} 1 \\ 0 \end{bmatrix}; \quad \mathbf{I}^z_{sh} = \begin{bmatrix} 0 \\ 1 \end{bmatrix}$$

On the other hand the four matrices $\mathbf{S}$, recalling the expression given in Tab. 4.1, can be expressed as follow:

$$\begin{aligned} \mathbf{S}^y_{lt} &= -\left(\mathbf{G}^T_y\ \mathbf{G}_\phi + \mathbf{G}^T_\phi\ \mathbf{G}_y\right) \\ \mathbf{S}^z_{lt} &= \mathbf{G}^T_z\ \mathbf{G}_\phi + \mathbf{G}^T_\phi\ \mathbf{G}_z \\ \mathbf{S}^y_{sh} &= \mathbf{G}^T_z\ \mathbf{N}_\phi + \mathbf{N}^T_\phi\ \mathbf{G}_z \\ \mathbf{S}^z_{sh} &= -\left(\mathbf{G}^T_y\ \mathbf{N}_\phi + \mathbf{N}^T_\phi\ \mathbf{G}_y\right) \end{aligned} \tag{5.9}$$

The dependency of $l_{2,lt}(\mathbf{u})$ from y and z has been overcome linking the the operator to the curvature and not directly to the axial strain. The expression given by Eq. (5.9) ensure the symmetry of all four $\mathbf{S}$ matrices [Jesper Dencker Larsen, 2007].

Bilinear operator

Same considerations made for the quadratic operator can be done for the bilinear operator. Below is given a summary of the expressions for the bilinear operator related with the three different non-linear effect.

$$l_{11}(\mathbf{u}_a,\mathbf{u}_b) = l_{11,eu}(\mathbf{u}_a,\mathbf{u}_b) + l_{11,ft}(\mathbf{u}_a,\mathbf{u}_b) + l_{11,lt}(\mathbf{u}_a,\mathbf{u}_b) \tag{5.10}$$

where:

$$\begin{aligned} l_{11,eu}(\mathbf{u}_a,\mathbf{u}_b) &= \mathbf{I}_{eu}\overline{\mathbf{V}}_a\ \mathbf{S}_{eu}\ \overline{\mathbf{V}}_b \\ l_{11,ft}(\mathbf{u}_a,\mathbf{u}_b) &= \mathbf{I}_{ft}\overline{\mathbf{V}}_a\ \mathbf{S}_{ft}\ \overline{\mathbf{V}}_b \end{aligned} \tag{5.11}$$

$$l_{11,lt}(\mathbf{u}_a,\mathbf{u}_b) \Rightarrow \begin{cases} l^c_{11,lt}(\mathbf{u}_a,\mathbf{u}_b) = \mathbf{I}^y_{lt}\ \overline{\mathbf{V}}^T_a\mathbf{S}^y_{ft}\ \overline{\mathbf{V}}_b + \mathbf{I}^z_{lt}\ \overline{\mathbf{V}}^T_a\mathbf{S}^z_{ft}\ \overline{\mathbf{V}}_b \\ l^s_{11,lt}(\mathbf{u}_a,\mathbf{u}_b) = \mathbf{I}^y_{sh}\ \overline{\mathbf{V}}^T_a\mathbf{S}^y_{sh}\ \overline{\mathbf{V}}_b + \mathbf{I}^z_{sh}\ \overline{\mathbf{V}}^T_a\mathbf{S}^z_{sh}\ \overline{\mathbf{V}}_b \end{cases} \tag{5.12}$$

$l_{11,eu}(\mathbf{u}_a,\mathbf{u}_b)$	Bilinear operator for euler effect
$l_{11,ft}(\mathbf{u}_a,\mathbf{u}_b)$	Bilinear operator for flexural-torsional effect
$l^c_{11,lt}(\mathbf{u}_a,\mathbf{u}_b)$	Bilinear operator for lateral-torsional effect (Curvature)
$l^s_{11,lt}(\mathbf{u}_a,\mathbf{u}_b)$	Bilinear operator for lateral-torsional effect (Shear)

The expand forms of the matrices can be found in the Appendix. B

5.1.2 Strain and stresses definitions

As was previously mentioned, shear strains and stresses are not directly included in the FEM formulation and they will be therefore defined separately.

Bernoulli beam fields

According to the Bernoulli beam theory the strain and stress field, with the operator definitions given in the previous section, can be define as:

$$\begin{aligned} &\boldsymbol{\sigma} = \mathbf{D}\boldsymbol{\varepsilon} \\ &\boldsymbol{\varepsilon} = l_1(\mathbf{u}) + \tfrac{1}{2}\left[l_{2,eu}(\mathbf{u}) + l_{2,ft}(\mathbf{u}) + l^c_{2,lt}(\mathbf{u})\right] \\ &\delta\boldsymbol{\varepsilon} = l_1(\delta\mathbf{u}) + \left[l_{11,eu}(\mathbf{u},\delta\mathbf{u}) + l_{11,ft}(\mathbf{u},\delta\mathbf{u}) + l^c_{11,lt}(\mathbf{u},\delta\mathbf{u})\right] \end{aligned} \tag{5.13}$$

The constitutive matrix $\mathbf{D}$, for a 3-D beam element can be written in an expand form as:

$$\mathbf{D} = \begin{bmatrix} EA & 0 & 0 & 0 & 0 \\ 0 & EI_z & 0 & 0 & 0 \\ 0 & 0 & EI_y & 0 & 0 \\ 0 & 0 & 0 & GI_t & 0 \\ 0 & 0 & 0 & 0 & EI_{ww} \end{bmatrix} \tag{5.14}$$

G	Shear modulus	$[Pa]$
I_t	Torsional constant	$[m^4]$
I_{ww}	Warping constant	$[m^6]$

Using the constitutive matrix expressed by Eq. (5.14), the stress field will be describe by a vector $[5 \times 1]$, which is composed as follow:

$$\boldsymbol{\sigma} = \begin{bmatrix} N \\ M_z \\ M_y \\ M_t \\ Bi \end{bmatrix} \tag{5.15}$$

N	Normal force	$[N]$
M_z	Bending moment around z-axis	$[Nm]$
M_y	Bending moment around y-axis	$[Nm]$
M_t	de Saint-Venant torsional moment	$[Nm]$
Bi	Bi-moment	$[Nm]$

Since beam elements are considered, the stress vectors will be actually composed by the internal forces as shown by Eq. (5.15).

Shear fields

The fields related to the shear can be expressed as:

$$\begin{aligned} \boldsymbol{\tau} &= \begin{bmatrix} V_y \\ V_z \end{bmatrix} = \mathbf{D}_{sh}\mathbf{B}_{sh}\overline{\mathbf{V}} \\ \boldsymbol{\gamma}_{n-lin} &= \begin{bmatrix} \gamma_{xy} \\ \gamma_{xz} \end{bmatrix} = l^s_{2,lt}(\mathbf{u}) \end{aligned} \tag{5.16}$$

$\boldsymbol{\gamma}_{n-lin}$	Non-linear shear strain vector
$\boldsymbol{\tau}$	Non-linear shear stress vector
V_y	Shear force along y-axis
V_z	Shear force along z-axis
$\mathbf{D}_{sh}$	Shear constitutive matrix
$\mathbf{B}_{sh}$	Shear interpolation matrix

The matrices $\mathbf{D}_{sh}$ and $\mathbf{B}_{sh}$, are artificial matrices build to define the shear forces; more specifically:

$$\begin{aligned} \mathbf{D}_{sh} &= \begin{bmatrix} 0 & EI_z & 0 & 0 & 0 \\ 0 & 0 & EI_y & 0 & 0 \end{bmatrix} \\ \mathbf{B}_{sh} &= \begin{bmatrix} \mathbf{G}_{y,xx} \\ \mathbf{G}_{z,xx} \end{bmatrix} \end{aligned} \tag{5.17}$$

Now that all the static variables are defined it is possible to proceed with the FEM implementation.

5.2 3-D FEM and the asymptotic postbuckling model

As a study-case to illustrate the employed procedure, a steel frame will be used. The specifics are shown in the following. The governing equation expressed in Chapter 4.3 are used, putting particular attention to include the shear strain and stress when it is needed.

5.2.1 Structure description

The analyzed frame is pictured in Fig 5.2.

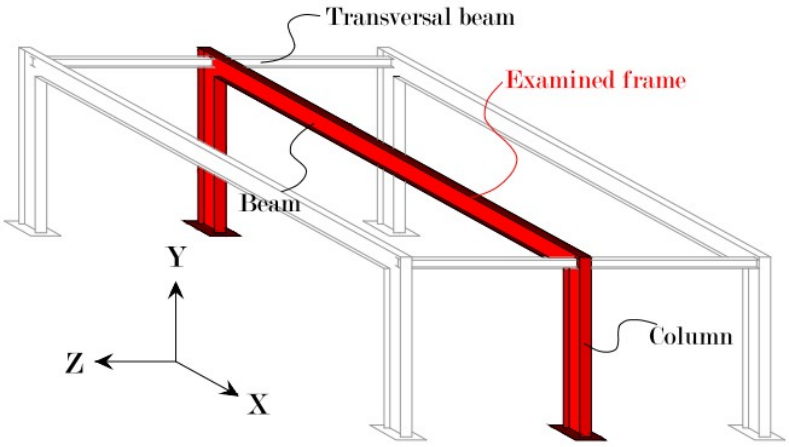

Figure 5.2. Frame 3-D [Carlos Luis Badillo Bercebal, 2014]

The columns have a span of 3 $[m]$ while the beam a span of 6. The frame is discretized using four element per meter, for a total number of element of 48 as pictured below.

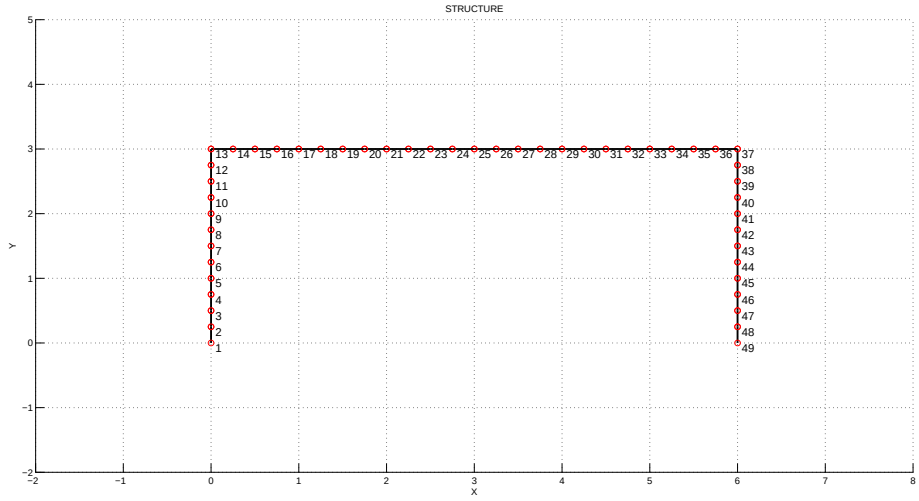

Figure 5.3. Frame discretization

The cross section used for both column and beam is a commercial I-profile called HEA100A, which geometric specifics are found in Appendix A.
Regarding the boundary conditions, instead, they are imposed as described in the following:

- **Static boundary condition**. The load is a linear distributed load q along the global y axis with a magnitude of -1 $[N/m]$ and is applied on the entire length of the beam. For simplicity it is considered applied along the beam axis at the elastic center of the cross section.

- **Kinematic boundary condition**. The kinematic boundary condition are depicted in Fig. 5.4.

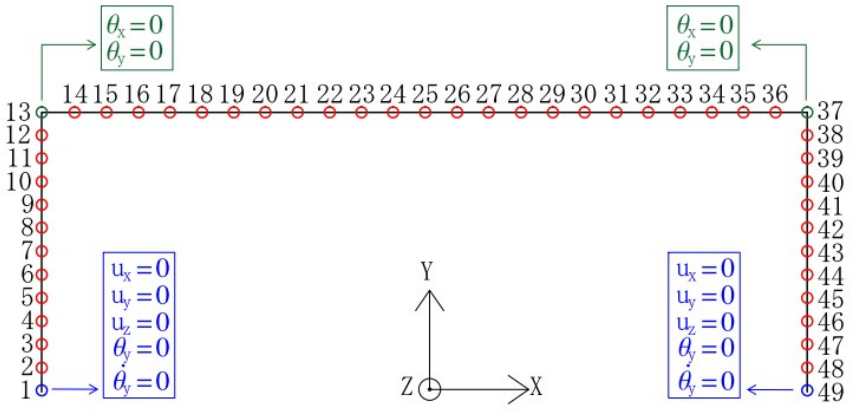

Figure 5.4. Kinematic boundary condition

The frame is pinned at the ground allowing only the bending of the columns. Furthermore at the corners torsion is constrained for both beam and columns. This is due to the presence of the transverse beam connecting the beam to the others frame of the structure as pictured in Fig. 5.2. A more detailed information about the boundary condition can be found in [Carlos Luis Badillo Bercebal, 2014].

5.2.2 Zero-order problem

The first step in the implementation of the asymptotic postbuckling model is to solve the zero-order problem. In the zero-order problem an elastic analysis is performed, and the governing equation is:

$$\boldsymbol{\sigma}_0 \cdot l_1(\delta\mathbf{u}) = R \cdot \delta\mathbf{u} \tag{5.18}$$

Eq. (5.18) can be written in a FE environment as:

$$\mathbf{K}\ \overline{\mathbf{V}}_0 = \overline{\mathbf{F}}_0 \tag{5.19}$$

The results for the studied frame is depicted in Fig. 5.5.

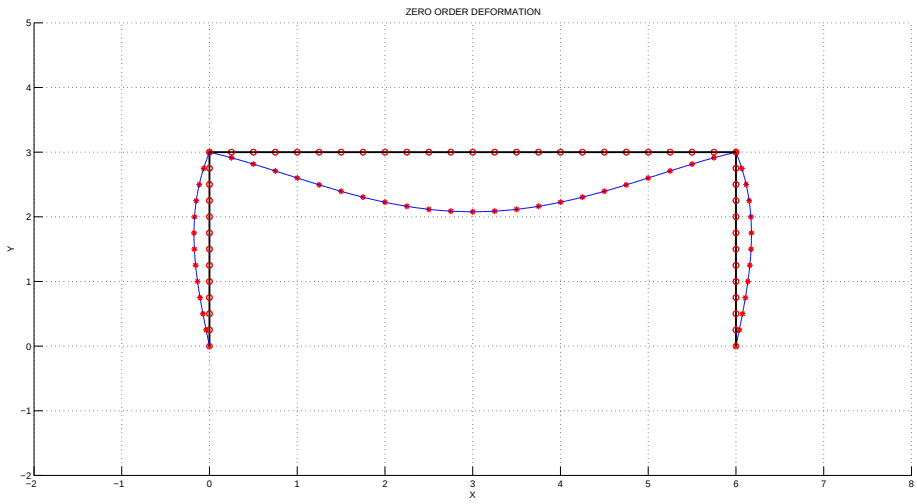

Figure 5.5. Zero-order deformation

The displacement field pictured in Fig. 5.5 is scaled with a scale factor of 10^5.
Once the displacement field $\overline{\mathbf{V}}_0$ is found, the internal forces vectors $\boldsymbol{\sigma}_0$ and $\boldsymbol{\tau}_0$ can be found by means of Eq. (5.13); more specifically:

$$\begin{cases} \boldsymbol{\varepsilon}_0 = \mathbf{B}\overline{\mathbf{V}}_0 & \Rightarrow \quad \boldsymbol{\sigma}_0 = \mathbf{D}\boldsymbol{\varepsilon}_0 \\ \boldsymbol{\gamma}_0 = \mathbf{B}_{sh}\overline{\mathbf{V}}_0 & \Rightarrow \quad \boldsymbol{\tau}_0 = \mathbf{D}_{sh}\boldsymbol{\gamma}_0 \end{cases} \tag{5.20}$$

The zero-order stress fields are needed for the solution of the higher order problems.

5.2.3 First order problem

Once the zero-order problem has been solved, the next step is to include the first order terms in the analysis. In this phase the critical load coefficient λ_c will be found and the

two displacement field related with the bifurcation point will be obtained. The governing equation of the first order problem, recalling the equation given in Tab. 4.1, is:

$$\boldsymbol{\sigma}_1 \cdot l_1(\delta\mathbf{u}) + \lambda_c \, \boldsymbol{\sigma}_0 \cdot l_{11}(\mathbf{u}_1,\delta\mathbf{u}) = 0 \tag{5.21}$$

Eq. (5.21) in FEM become:

$$(\mathbf{K} + \lambda_c \mathbf{K}_g)\, \overline{\mathbf{V}}_1 = 0 \tag{5.22}$$

The stress stiffness matrix $\mathbf{K}_g$ is obtained by a volume integration of the product $[\boldsymbol{\sigma}_0 \cdot l_{11}(\mathbf{u}_1,\delta\mathbf{u})]$ and therefore can be divided pointing out the three different effect by means of Eq. (5.10). Hence the stress stiffness matrix can be expressed as:

$$\mathbf{K}_g = \mathbf{K}_g^{eu} + \mathbf{K}_g^{ft} + \mathbf{K}_g^{lt} \tag{5.23}$$

$\mathbf{K}_g^{eu}$	Stress stiffness matrix for euler buckling effect
$\mathbf{K}_g^{ft}$	Stress stiffness matrix for flexural-torsional effect
$\mathbf{K}_g^{lt}$	Stress stiffness matrix for lateral-torsional effect

All the matrix definitions in the following are given for one beam element. The global matrix $\mathbf{K}_g$ will be assembled in the same manner as the stiffness matrix $\mathbf{K}$.
The matrix $\mathbf{K}_g^{eu}$ is obtained as follow[2] [Jesper Dencker Larsen, 2007]:

$$\mathbf{K}_g^{eu} = \int_V |\mathbf{I}_{eu}\boldsymbol{\sigma}_0| \;\; \mathbf{S}_{eu} \; dV \tag{5.24}$$

The volume integration expressed by Eq.(5.24) can be reduced to a line integration in the local coordinate ξ. The reduction entail that the only non zero term will be the one related to the normal stress; i.e. normal internal force N_0. This is because the integration over the cross section of normal stress connected to the bending moment will be equal to zero due to its symmetric distribution [Jesper Dencker Larsen, 2007]. After some deception, the stress stiffness matrix $\mathbf{K}_g^{eu}$ can be expressed as:

$$\mathbf{K}_g^{eu} = \int_{-1}^{1} N_0 \; \mathbf{S}_{eu} \; J d\xi \tag{5.25}$$

Furthermore the stress stiffness matrix $\mathbf{K}_g^{ft}$ can be expressed in a similar way as the matrix $\mathbf{K}_g^{eu}$; more specifically [Jesper Dencker Larsen, 2007]:

$$\mathbf{K}_g^{ft} = \int_V |\mathbf{I}_{ft}\boldsymbol{\sigma}_0| \;\; \mathbf{S}_{ft} \; dV \tag{5.26}$$

With similar consideration made for $\mathbf{K}_g^{eu}$, also in this case the integral can be reduced and after some deceptions the following expression is obtained:

$$\mathbf{K}_g^{ft} = \frac{I_z + I_y}{A} \;\; \int_{-1}^{1} N_0 \; \mathbf{G}_\phi^T \mathbf{G}_\phi \; J d\xi \tag{5.27}$$

[2] A local coordinate ξ has been used as in the 2-D case

The presence of the coefficient $\frac{I_z+I_y}{A}$ is due to the integration of the coordinate y and z (see [Jesper Dencker Larsen, 2007]).
The last matrix to define is the one related to the lateral-buckling effect. This is the case where the shear effect has to be taken into account. Hence the matrix $\mathbf{K}_g^{lt}$ can be expressed, according to Eq. (5.12), as:

$$\mathbf{K}_g^{lt} = \int_V \left[|\mathbf{I}_{lt}^y \boldsymbol{\sigma}_0| \ \mathbf{S}_{lt}^y + |\mathbf{I}_{lt}^z \boldsymbol{\sigma}_0| \ \mathbf{S}_{lt}^z + |\mathbf{I}_{sh}^y \boldsymbol{\tau}_0| \ \mathbf{S}_{sh}^y + |\mathbf{I}_{sh}^z \boldsymbol{\tau}_0| \ \mathbf{S}_{sh}^z \right] \ dV \tag{5.28}$$

Also in this case, the integration can be reduced to a linear integral. Nevertheless in the integration expressed by Eq. (5.28) is not the normal force who gives the non zero contribution but are the bending moments and the shear forces instead. Hence the following expression for the matrix $\mathbf{K}_g^{lt}$ is obtained [Jesper Dencker Larsen, 2007].

$$\mathbf{K}_g^{lt} = \int_V \left[M_{z0} \ \mathbf{S}_{lt}^y + M_{y0} \ \mathbf{S}_{lt}^z + V_{y0} \ \mathbf{S}_{sh}^y + V_{z0} \ \mathbf{S}_{sh}^z \right] \ J d\xi \tag{5.29}$$

The stress stiffness matrix $\mathbf{K}_g^{lt}$ is obtained by means of Eq. (5.9) and (5.29). Furthermore has to be noticed that the shear forces V_{y0} and V_{z0} are constant over the element, while the moments M_{y0} and M_{z0} have a linear variation; i.e. they have to be integrated.
Once the global stress stiffness matrix $\mathbf{K}_g$ is defined, the eigenvalue problem expressed by Eq. (5.22) can be solved. For the studied frame, the critical load coefficient λ_c shown in Tab 5.1 is obtained.

λ_c	13925.9215

Table 5.1. Critical load coefficient

The displacement fields related to the bifurcation point are depicted in Fig. 5.6 and Fig. 5.7.

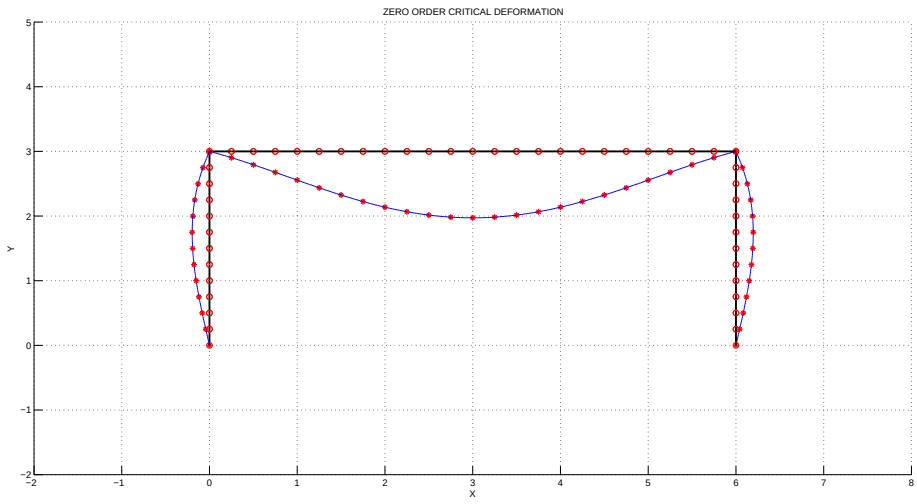

Figure 5.6. Zero-order bifurcation point displacement field

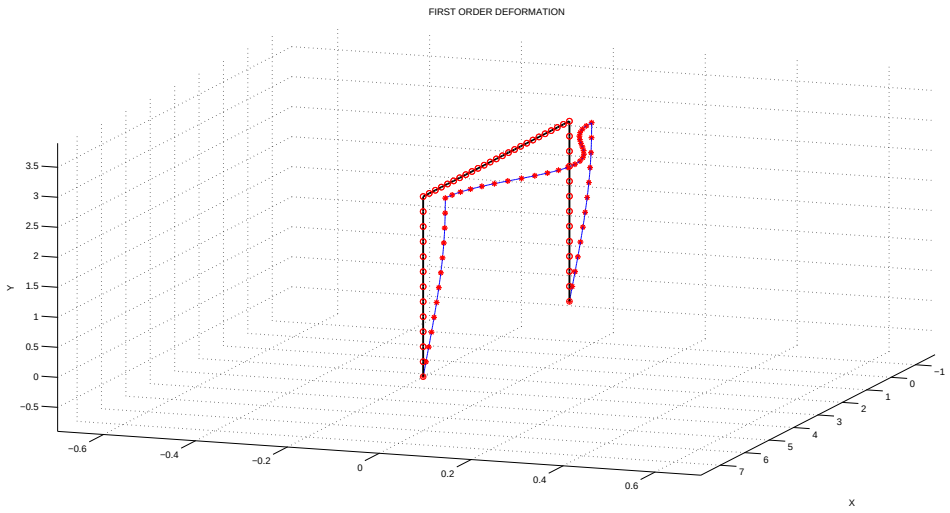

Figure 5.7. First order buckling mode

The displacement fields pictured in Fig. 5.6 and 5.7 are scaled respectively with a factor of 4 and 8. As it can be seen the buckling mode consist mainly in a deflection of the beam around the global y-axis which represent weak axis for the considered structural element. Stress and strain field can be obtained as shown below.

$$\begin{cases} \boldsymbol{\varepsilon}_1 = \mathbf{B}\overline{\mathbf{V}}_1 & \Rightarrow \quad \boldsymbol{\sigma}_1 = \mathbf{D}\boldsymbol{\varepsilon}_1 \\ \boldsymbol{\gamma}_1 = \mathbf{B}_{sh}\overline{\mathbf{V}}_1 & \Rightarrow \quad \boldsymbol{\tau}_1 = \mathbf{D}_{sh}\boldsymbol{\gamma}_1 \end{cases} \tag{5.30}$$

First order local correction

As for the two dimensional case, in order to obtain a more reliable result a correction for both bending moments has to be applied. The procedure is the same described in Chapter 3.2.3 and therefore an extra four d.o.f. will be added locally as depicted in Fig. 5.8. For the torsional d.o.f*s*, instead, no correction has been applied.

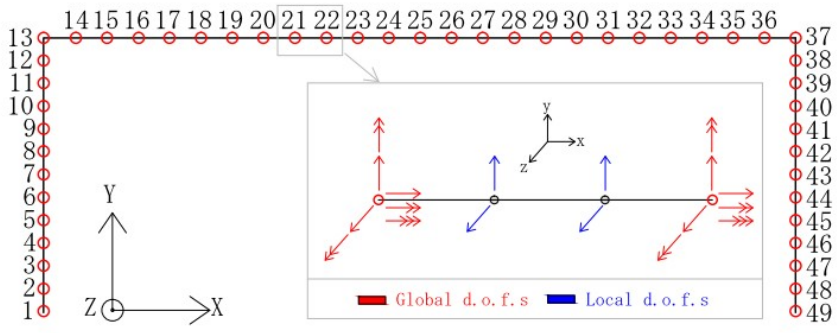

Figure 5.8. First order correction: 3-D

The local increment of d.o.f leads to a fifth order polynomial variation of the displacement

along the local y and z axis; i.e. the correction will affect also the shear forces, since they are calculated as a derivative of the bending moments. Hence the shear forces will follow a linear variation while the bending moments will follow a parabolic variation. The governing FE equation for the local problem is:

$$\mathbf{K}_l \overline{\mathbf{V}}_{1l} = -\lambda_c \mathbf{K}_{gl} \overline{\mathbf{V}}_1 \tag{5.31}$$

The local matrices are calculated using local shape functions. More specifically the matrix $\mathbf{K}_{gl}$ is assembled using a local $\mathbf{S}_l$ matrix which can be generally defined as:

$$\begin{aligned} \mathbf{S}_l &= \mathbf{G}_l^T \mathbf{G} \\ \mathbf{S}_l^{sh} &= \mathbf{G}_l^T \mathbf{N} \end{aligned} \tag{5.32}$$

Applying Eq. (5.32) to each one of the $\mathbf{S}$ matrix provided in Chapter 5.1.1, allow to determine the local stress stiffness matrix $\mathbf{K}_{gl}$. In the determination of $\mathbf{K}_{gl}$ a particular attention has to be put since neither shear forces nor bending moments are constant and therefore are both subjected to integration. Hence solving Eq. (5.31), the first order local displacement field $\overline{\mathbf{V}}_{1l}$ is obtained and the corrected stress fields can be calculated as follow.

$$\begin{cases} \boldsymbol{\sigma}_{1l} = \mathbf{D}\ \mathbf{B}_l \overline{\mathbf{V}}_{1l} & \Rightarrow \quad \boldsymbol{\sigma}_{1tot} = \boldsymbol{\sigma}_1 + \boldsymbol{\sigma}_{1l} \\ \boldsymbol{\tau}_{1l} = \mathbf{D}_{sh}\ \mathbf{B}_{l,sh} \overline{\mathbf{V}}_{1l} & \Rightarrow \quad \boldsymbol{\tau}_{1tot} = \boldsymbol{\tau}_1 + \boldsymbol{\tau}_{1l} \end{cases} \tag{5.33}$$

The first order stress fields together with the zero-order stress fields allow to proceed with the solution of the second, and consequently, the third order problem.

5.2.4 Second order problem

The first step in the solution of the second order problem, is the determination of the first buckling coefficient a. Recalling the expression previously given in Chapter 2.2.3, the a coefficient can be written as:

$$a = -\frac{1}{\lambda_c}\ \frac{3}{2}\ \frac{\boldsymbol{\sigma}_1 \cdot l_2(\mathbf{u}_1)}{\boldsymbol{\sigma}_0 \cdot l_2(\mathbf{u}_1)} \tag{5.34}$$

As it is shown by Eq. (5.34), the determination of the a coefficient involve the product between stress field and quadratic operator. Therefore it is necessary to include also the shear's effects, which lead to an expression for the first buckling coefficient in a FE environment such as:

$$a = -\frac{1}{\lambda_c}\ \frac{3}{2}\ \frac{\sum_{i=1}^{n} \int \left\{ \boldsymbol{\sigma}_{1tot} \cdot \left[l_{2,eu}(\mathbf{u}_1) + l_{2,ft}(\mathbf{u}_1) + l^c_{2,lt}(\mathbf{u}_1) \right] + \boldsymbol{\tau}_{1tot} \cdot l^s_{2,lt}(\mathbf{u}_1) \right\} \cdot J d\xi}{\sum_{i=1}^{n} \int \left\{ \boldsymbol{\sigma}_0 \cdot \left[l_{2,eu}(\mathbf{u}_1) + l_{2,ft}(\mathbf{u}_1) + l^c_{2,lt}(\mathbf{u}_1) \right] + \boldsymbol{\tau}_0 \cdot l^s_{2,lt}(\mathbf{u}_1) \right\} \cdot J d\xi} \tag{5.35}$$

Eq. (5.35), together with the operator definition given in Chapter 5.1.1, convey to the value of the first buckling coefficient reported in Tab. 5.2.

a	$-3.0529 \times 10^{-15} \cong 0$

Table 5.2. First buckling coefficient a

A value of 0 was expected due to the symmetry of the studied frame.
Once the value of the first buckling coefficient is found, it is possible to proceed with the solution of the second order problem. The governing equation of the second order problem, recalling the equation given in Tab. 4.1, is:

$$\boldsymbol{\sigma}_2^{'} \cdot l_1(\delta\mathbf{u}) + \lambda_c \boldsymbol{\sigma}_0 \cdot l_{11}(\mathbf{u}_2,\delta\mathbf{u}) = -[\underbrace{(a\lambda_c\boldsymbol{\sigma}_0 + \boldsymbol{\sigma}_1) \cdot l_{11}(\mathbf{u}_1,\delta\mathbf{u})}_{L_1} + \underbrace{\boldsymbol{\sigma}_2^{''} \cdot l_1(\delta\mathbf{u})}_{L_2}] \tag{5.36}$$

Eq. (5.36) can be translate in a FE language as:

$$(\mathbf{K} + \lambda_c \mathbf{K}_g) \cdot \overline{\mathbf{V}}_2 = -(\overline{\mathbf{L}}_1 + \overline{\mathbf{L}}_2) \tag{5.37}$$

$\overline{\mathbf{L}}_1$, $\overline{\mathbf{L}}_2$ | Second order laod vectors

The load vectors $\overline{\mathbf{L}}_1$ and $\overline{\mathbf{L}}_2$, using the operators definitions given in Chapter 5.1.1, can be written as:

$$\begin{aligned}
\overline{\mathbf{L}}_1 &= \int \left\{ (a\lambda_c\boldsymbol{\sigma}_0 + \boldsymbol{\sigma}_{1tot}) \cdot \left[l_{11,eu}(\mathbf{u}_1,\delta\mathbf{u}) + l_{11,ft}(\mathbf{u}_1,\delta\mathbf{u}) + l^c_{11,lt}(\mathbf{u}_1,\delta\mathbf{u}) \right] + \boldsymbol{\tau}_{1tot} \cdot l^s_{11,lt}(\mathbf{u}_1,\delta\mathbf{u}) \right\} \cdot Jd\xi \\
\overline{\mathbf{L}}_2 &= \int \left\{ \tfrac{1}{2}\mathbf{B}^T\mathbf{D} \cdot \left[l_{2,eu}(\mathbf{u}_1) + l_{2,ft}(\mathbf{u}_1) + l^c_{2,lt}(\mathbf{u}_1) \right] \right\} \cdot Jd\xi
\end{aligned} \tag{5.38}$$

In the definition of the load vector $\overline{\mathbf{L}}_2$ given by Eq. (5.38), the shear contribution has not been included. This is due to the fact that even though there is a non-linear shear stress, the linear operator defining the linear shear strain is considered equal to 0 since linear shear strain are neglected. Furthermore, as in the 2-D case, the left-hand side of Eq. (5.37) is singular. Hence in order to solve the second order problem it is necessary to: [Poulsen and Damkilde, 1998]

- Apply an extra kinematic boundary condition
- Apply an orthogonality condition between $\mathbf{u}_1$ and $\mathbf{u}_2$

The additional kinematic boundary condition is applied where $\overline{\mathbf{V}}_1$ has its maximum value. Eq. (5.37) can now be solved and the second order dislpacement field $\widetilde{\mathbf{V}}_2$ is found. Therefore the orthogonality condition, recalling Eq. (3.25), is applied by means of the following expression.

$$\overline{\mathbf{V}}_2 = \widetilde{\mathbf{V}}_2 - \frac{\overline{\mathbf{V}}_1^T \, \mathbf{K}\widetilde{\mathbf{V}}_2}{\overline{\mathbf{V}}_1^T \, \mathbf{K}\overline{\mathbf{V}}_1} \, \overline{\mathbf{V}}_1$$

The second order displacement field $\overline{\mathbf{V}}_2$ is then obtained and it is depicted in Fig. 5.9.

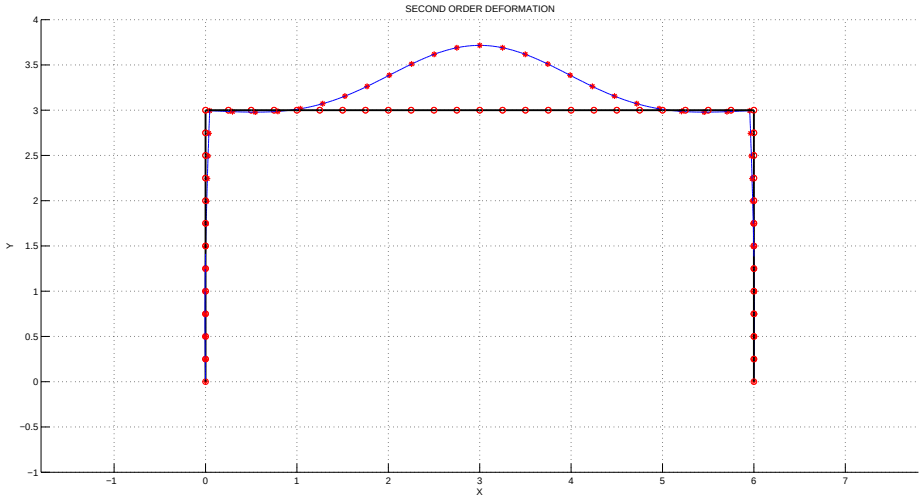

Figure 5.9. Second order displacement field

The displacement field pictured in Fig. 5.9 is scaled with a scale factor of 10^3.
From the displacement field $\overline{\mathbf{V}}_2$, the strain and stress fields are obtained as follow:

$$\begin{cases} \boldsymbol{\varepsilon}_2 = l_1(\mathbf{u}_2) + \frac{1}{2}\left[l_{2,eu}(\mathbf{u}_1) + l_{2,ft}(\mathbf{u}_1) + l^c_{2,lt}(\mathbf{u}_1)\right] & \Rightarrow \quad \boldsymbol{\sigma}_2 = \mathbf{D}\boldsymbol{\varepsilon}_2 \\ \boldsymbol{\gamma}_2 = \mathbf{B}_{sh}\overline{\mathbf{V}}_2 & \Rightarrow \quad \boldsymbol{\tau}_2 = \mathbf{D}_{sh}\boldsymbol{\gamma}_2 \end{cases} \tag{5.39}$$

Second order correction

The second order correction, as in the 2-D case, is applied to obtained a more reliable result of the second buckling coefficient b. Besides the first order correction, which affect the bending moments, a second order correction affecting the normal stresses will be introduced. The second order correction is applied following the same procedure employed for the 2-D elements and therefore an additional four axial d.o.f*s* are applied locally on the elements as depicted in Fig. 5.10. Furthermore a fifth order polynomial variation is used to interpolate the displacement along the local x axis.

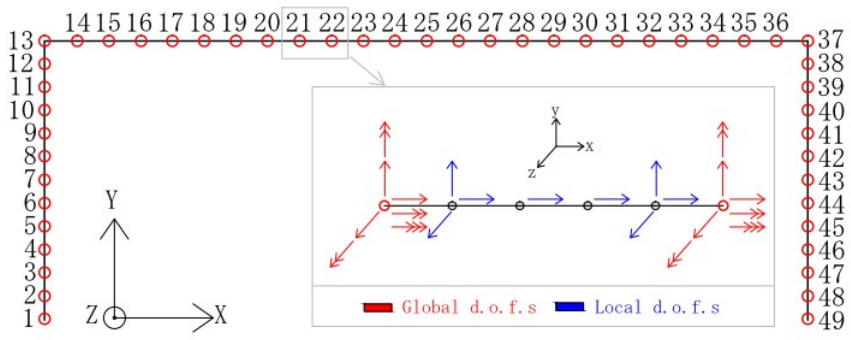

Figure 5.10. Second order correction: 3-D

A summary of the interpolation's polynomial are reported below[3].

$$\begin{array}{lcl} u_x & \Rightarrow & 5th \text{ order polyniomial} \\ u_y & \Rightarrow & 5th \text{ order polyniomial} \\ u_z & \Rightarrow & 5th \text{ order polyniomial} \\ \phi & \Rightarrow & 3rd \text{ order polyniomial} \end{array}$$

The governing FE equation for the second order local problem is:

$$\mathbf{K}_l \overline{\mathbf{V}}_{2l} = -(\overline{\mathbf{L}}_{1l} + \overline{\mathbf{L}}_{2l} + \lambda_c \mathbf{K}_{gl} \overline{\mathbf{V}}_2) \tag{5.40}$$

$\overline{\mathbf{L}}_{1l}$, $\overline{\mathbf{L}}_{2l}$ | Second order local load vectors

As for the matrix $\mathbf{K}_{gl}$ in the first order correction, also the local load vector $\overline{\mathbf{L}}_{1l}$ is found defining local operators by means of a local matrix $\mathbf{S}$ obtained as shown by Eq. (5.32). On the other hand the local load vector $\overline{\mathbf{L}}_{2l}$ is obtained as follow.

$$\overline{\mathbf{L}}_{2l} = \int \left\{ \frac{1}{2} \mathbf{B}_l^T \mathbf{D} \cdot \left[l_{2,eu}(\mathbf{u}_1) + l_{2,ft}(\mathbf{u}_1) + l^c_{2,lt}(\mathbf{u}_1) \right] \right\} \cdot J d\xi \tag{5.41}$$

As shown by Eq. (5.41), the local load vector $\overline{\mathbf{L}}_{2l}$ is obtained by means of the local interpolation matrix $\mathbf{B}_l$. The solution to Eq. (5.40) leads to the local displacement field $\overline{\mathbf{V}}_{2l}$, and the second order stress correction is obtained as follow.

$$\begin{cases} \boldsymbol{\sigma}_{2l} = \mathbf{D}\ \mathbf{B}_l \overline{\mathbf{V}}_{2l} & \Rightarrow \quad \boldsymbol{\sigma}_{2tot} = \boldsymbol{\sigma}_2 + \boldsymbol{\sigma}_{2l} \\ \boldsymbol{\tau}_{2l} = \mathbf{D}_{sh}\ \mathbf{B}_{l,sh} \overline{\mathbf{V}}_{2l} & \Rightarrow \quad \boldsymbol{\tau}_{2tot} = \boldsymbol{\tau}_2 + \boldsymbol{\tau}_{2l} \end{cases} \tag{5.42}$$

Since the three stress fields $\boldsymbol{\sigma}_0$, $\boldsymbol{\sigma}_{1tot}$ and $\boldsymbol{\sigma}_{2tot}$ are found, it is now possible to proceed with the final step and calculate the second buckling coefficient

5.2.5 Third order problem

At the third order problem is connected the calculation of the second buckling coefficient b. The b-coefficient is define by the stress fields obtained from the previous problems and can be expressed, recalling Eq. (2.34), as:

$$b = -\frac{1}{\lambda_c} \frac{\boldsymbol{\sigma}_2 \cdot l_2(\mathbf{u}_2) + 2\boldsymbol{\sigma}_1 \cdot l_{11}(\mathbf{u}_1, \mathbf{u}_2)}{\boldsymbol{\sigma}_0 \cdot l_2(\mathbf{u}_1)} \tag{5.43}$$

The corresping FEM equation, can be written as:

$$b = -\frac{1}{\lambda_c} \frac{\sum_{i=1}^{n} (Num_{b1} + 2 \cdot Num_{b2})}{\sum_{i=1}^{n} Den_b} \tag{5.44}$$

[3]The displacement are expressed in the local coordinate system

The three terms Num_{b1} , Num_{b2} and Den_b are evaluated for each element and a summation over the total number of element is done. The expressions for the three terms are listed below.

$$\begin{cases} Num_{b1} = \int \left\{ \boldsymbol{\sigma}_{2tot} \cdot \left[l_{2,eu}(\mathbf{u}_2) + l_{2,ft}(\mathbf{u}_2) + l^c_{2,lt}(\mathbf{u}_2) \right] + \boldsymbol{\tau}_{2tot} \cdot l^s_{2,lt}(\mathbf{u}_2) \right\} \cdot Jd\xi \\ Num_{b2} = \int \left\{ \boldsymbol{\sigma}_{1tot} \cdot \left[l_{11,eu}(\mathbf{u}_1,\mathbf{u}_2) + l_{11,ft}(\mathbf{u}_1,\mathbf{u}_2) + l^c_{11,lt}(\mathbf{u}_1,\mathbf{u}_2) \right] + \boldsymbol{\tau}_{1tot} \cdot l^s_{11,lt}(\mathbf{u}_1,\mathbf{u}_2) \right\} \cdot Jd\xi \\ Den_b = \int \left\{ \boldsymbol{\sigma}_0 \cdot \left[l_{2,eu}(\mathbf{u}_2) + l_{2,ft}(\mathbf{u}_2) + l^c_{2,lt}(\mathbf{u}_2) \right] + \boldsymbol{\tau}_0 \cdot l^s_{2,lt}(\mathbf{u}_2) \right\} \cdot Jd\xi \end{cases} \tag{5.45}$$

Therefore the solution to Eq. (5.44), together with Eq. (5.45) and the operator's definitions given in Chapter 5.1.1, leads to a value for the b-coefficient that is:

b	-0.036806

Table 5.3. Second buckling coefficient b

The negative value of the second buckling coefficient suggest the the studied frame is unstable and therefore a quick drop of stiffness is expected after the bifurcation point. In order to validate this results a comparison will be done performing a non-linear analysis with ABAQUS.

5.3 ABAQUS Non-linear analysis: 3-D

Since there are not analytical results for the studied 3-D frame, a non-linear analysis using ABAQUS has been employed to validate the results obtained by mean of the asymptotic post buckling model. As was previously stated, 3-D beam element implemented in commercial program does not allow to include thin walled effects. Therefore to create a FE model closer to the one that has been analyzed, a 3-D model of the frame using shell element has been created as pictured below.

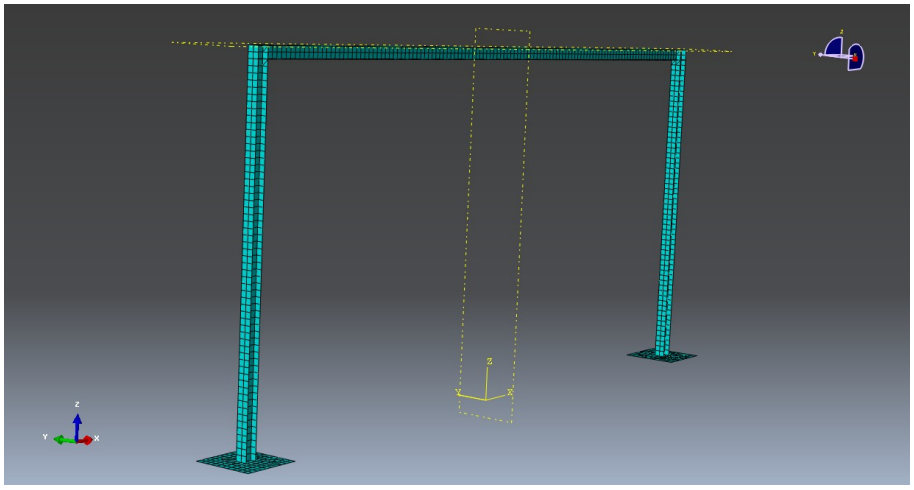

Figure 5.11. ABAQUS Frame model

The geometrical and material properties are the same used in the previous chapter but particular attention has to be put on the boundary condition.

Static boundary condition

In the ABAQUS model a pressure load of -10 $[N/m^2]$ has been applied on the upper flange of the beam as depicted in Fig. 5.12.

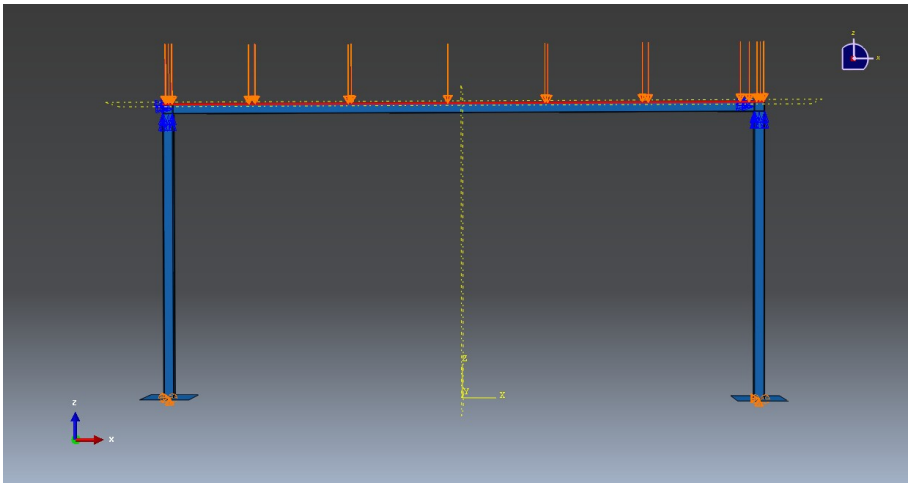

Figure 5.12. Static boundary condition

The pressure load will be equivalent to the line load applied on the Matlab model, since the flange has a width of 0.1 $[m]$. The fact that the load is applied on the upper will introduce an additional instability effect that is not been considered in the previous analysis. As a consequence, a smaller value of critical load factor is expected from the ABAQUS analysis.

Kinematic boundary condition

In order to simulate the boundary conditions imposed in the asymptotic FEM analysis, some precautions have to be taken. First of all the pin constrain at the end of the columns has been applied modeling a plate and restraining the the point on the cross section as shown in Fig. 5.13.

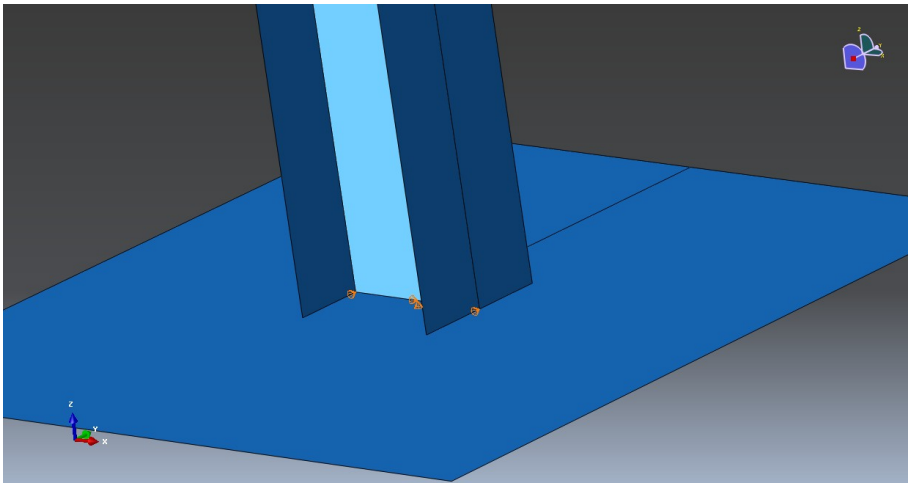

Figure 5.13. Pin constrain 3-D

The middle point of the web is constrained against the global x and y displacement while the end points are constrained against the displacement out of the frame plane in order to constrain torsion. The stiff plate has been added to constrain the warping of the cross section.
On the other hand, the torsional restrains for both beam and columns have been imposed on the highlighted lines pictured in Fig. 5.14. A more detailed explanation about the application of the boundaries condition can be found in [Carlos Luis Badillo Bercebal, 2014].

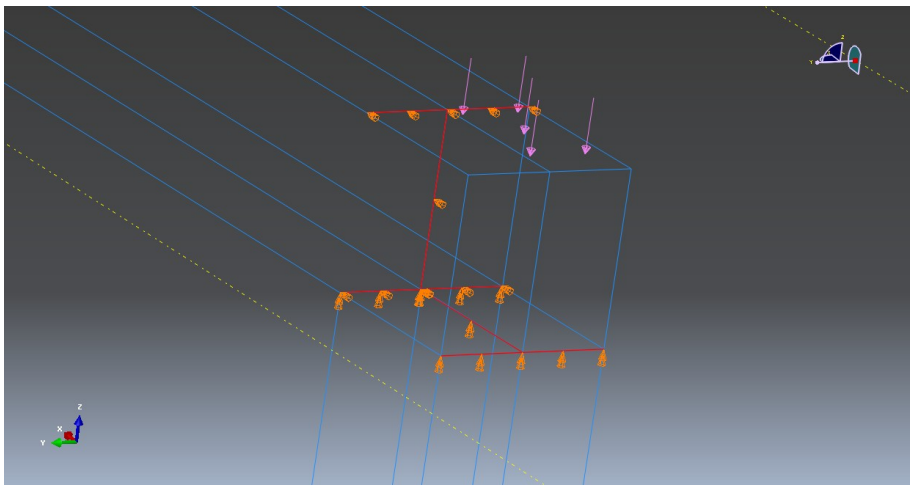

Figure 5.14. Corners constrain 3-D

To obtained the $\lambda - u$ relation the same steps followed in the 2-D analysis, have been employed.
At first the a buckling analysis is performed in order to obtain the critical load factor and the following results are obtained.

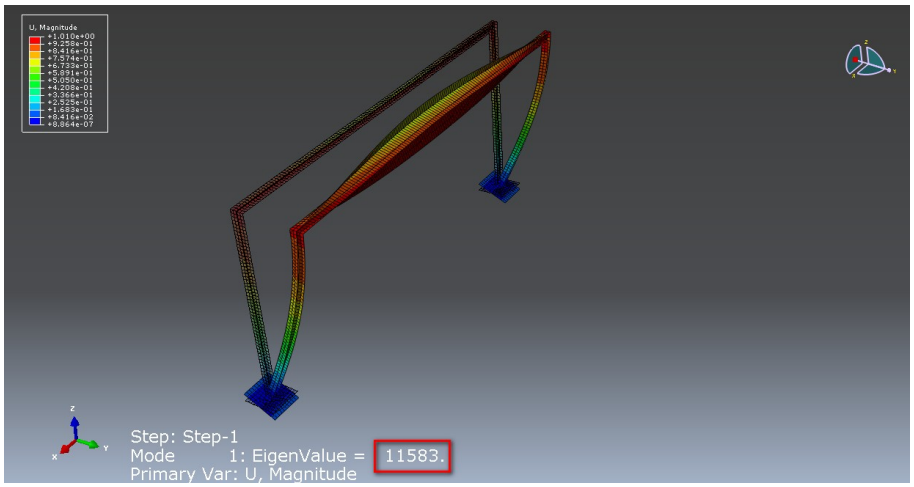

Figure 5.15. ABAQUS buckling mode: 3-D

	Matlab	ABAQUS
λ_c	13926	11583

Table 5.4. Critical load factors 3-D

The buckling mode depicted in Fig. 5.15 show a similar deformation out of the frame's plane as the one pictured in Fig. 5.7. Moreover, as it is shown in Tab. 5.4, the ABAQUS critical load factor result in a smaller value compered with the Matlab critical load factor, as was expected. At a later stage a non-linear analysis is performed following the same logic adopted for the 2-D analysis:

- The load applied is equal to -117000 $[N/m^2]$.

- The load increment is equal to 0.001

The matrix is symmetric and therefore non sensitive to imperfection. Hence to highlight the postbuckling behavior through a non-linear analysis it is necessary to include an initial imperfection. This has been done extruding the beam along a curved axis which have a maximum initial displacement of 0.01 $[m]$ at the middle point of the beam in the direction of the first buckling mode. The results depicted in Fig. 5.16 is obtained.

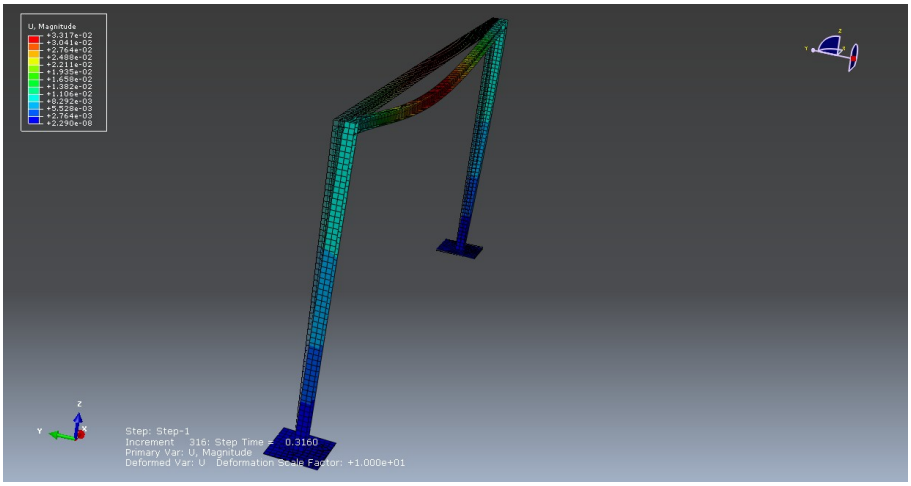

Figure 5.16. ABAQUS Non-linear: 3-D

To show the comparison between the non-linear analysis and the asymptotic analysis, the middle node of the beam has been chosen and the following results are obtained:

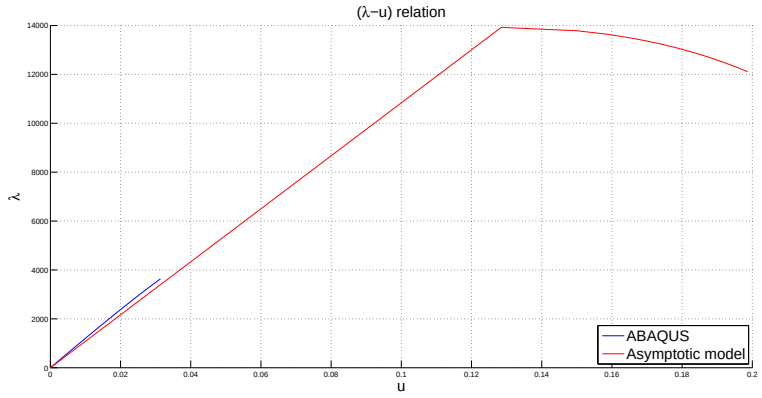

Figure 5.17. Load factor-displacement relation: 3-D

From Fig. 5.17 the following consideration can be done:

1. The non-linear analysis failed at a value of the critical load a lot smaller then the critical one. This could be due to a wrong setting of the initial imperfection. Nevertheless from a first analysis of the results depicted in Fig. 5.17, it can be infer that the frame is not sensitive to imperfection since the ABAQUS $\lambda - u$ relation seems to follow quite precisely the asymptotic one. Regarding the second buckling coefficient, a better non-linear analysis has to be employed in order to validate the buckling instability suggested by the asymptotic solution.

2. The solution obtained from the FE implementation of the asymptotic post buckling model, seems to correspond to the second case depicted in Fig. 2.1. This result seems quite reasonable as the two frames have similar static characteristics.

Conclusion 6

The asymptotic post buckling model has been implemented using both 2-D and 3-D elements. Different results have been achieved and the following conclusions can be done.

2-D Application

The finite element application of the asymptotic post buckling model using 2-D beam element, has shown that the model can predict quite well the imperfection sensitivity of and the postbuckling stability. The application to a simple case such as the Roodra's frame has confirmed that the FE implementation of the model leads to reliable results even though a relevant number of elements have to be used in order to reach convergence. Nevertheless the application of the stress corrections through the solution of a local problem with additional d.o.f, have the tendency to increase the computational power required for the solution. In fact when the convergence analysis has been employed, the time required to reach a solution drastically increased with the increment of the number of elements. On the other hand, the accuracy of the model in the analysis of a buckling phenomenon has be proved not only from the analytical results, but also from the non-linear static analysis performed by means of ABAQUS.

3-D Application

The application of the asymptotic postbuckling model to a 3-D FE problem, pointed out some complication related to the type of element that has been used. In fact the choice of the Bernoulli beam element has introduced some complication in the definition of the fields related to the different order problems. Because of the Bernoulli beam theory inconsistency regarding shear strains and stresses, has been necessary to introduce some further manipulation in order to obtain a more reliable stress fields. Since the two buckling coefficients strongly depend on the value of the stress fields, using Bernoulli beam elements could be a limit for the accuracy of the asymptotic model when it is applied to beam element. Therefore the choice of the Thimoshenko beam element would it be more appropriate for the application of the asymptotic postbuckling model. Nevertheless the results obtained analyzing the steel frame seem quite promising. Even though there any analytical results are available to validate the one obtained by the presented work, the value of the two coefficients appear to be reasonable considering the analyzed frame. In fact the 3-D frame has in principle the same static characteristics as the second case depicted below.

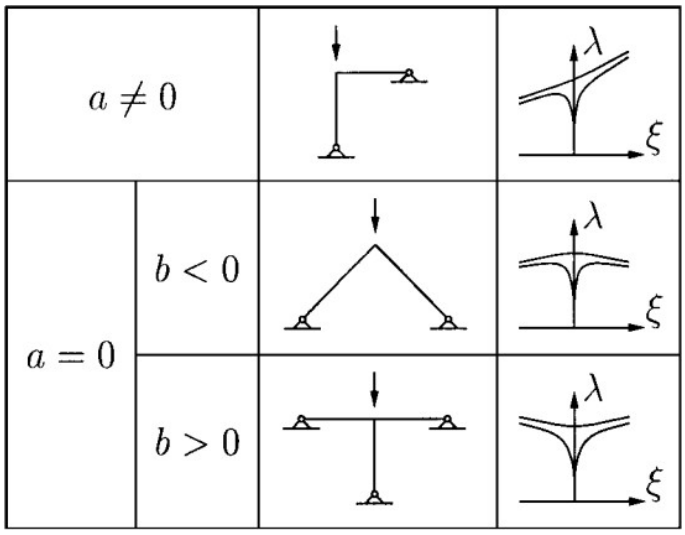

Figure 6.1. Buckling coef. and relative postbuckling behavior,[Poulsen and Damkilde, 1998]

If this is the case, it is reasonable that values of $a = 0$ and $b \leq 0$ are obtained.

6.1 Future developments

Few suggestions for future developments are reported in the following:

- Implementation of the asymptotic postbuckling model considering non-linear prebuckling beahviour;
- Implementation according to Thimoshenko beam theory;
- Extension of the model to other type of elements;
- Study of the modes interaction

Appendix A

The geometric specifics for the cross section HEA-100-A are listed in the following.

HE100A			
Geometry			
h = 96 mm	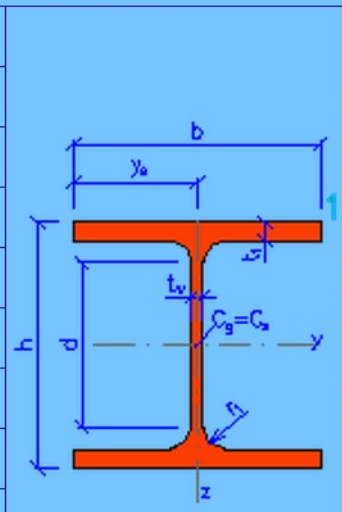	**Section properties**	
b = 100 mm		Axis y	Axis z
t_f = 8 mm		I_y = 3.49E+6 mm^4	I_z = 1.34E+6 mm^4
t_w = 5 mm		W_{y1} = 7.28E+4 mm^3	W_{z1} = 2.68E+4 mm^3
r_1 = 12 mm		$W_{y,pl}$ = 8.30E+4 mm^3	$W_{z,pl}$ = 4.11E+4 mm^3
y_s = 50 mm		i_y = 40.6 mm	i_z = 25.1 mm
d = 56 mm		S_y = 4.15E+4 mm^3	S_z = 2.06E+4 mm^3
A = 2124 mm^2		**Warping and buckling**	
A_L = 0.56 $m^2.m^{-1}$		I_w = 2.58E+9 mm^6	I_t = 5.24E+4 mm^4
G = 16.7 $kg.m^{-1}$		i_w = 23.11 mm	i_{pc} = 47.69 mm

Figure A.1. HEA100A

Appendix B

The definition of the matrices used in a FE implementation which adopt 3-D Bernoulli beam element are listed in the following.

B.1 Shape function standard element

The d.o.f*s* for each element are organized in the following oredr:

$$\begin{bmatrix} u_{x1} \\ u_{y1} \\ u_{z1} \\ \phi_1 \\ \theta_{y1} \\ \theta_{z1} \\ \dot{\phi}_1 \\ u_{x2} \\ u_{y2} \\ u_{z2} \\ \phi_2 \\ \theta_{y2} \\ \theta_{z2} \\ \dot{\phi}_2 \end{bmatrix} \tag{B.1}$$

According to [Cook et al., 2007], the shape function can be derived as:

$$\begin{aligned} \overline{\mathbf{X}}_{ax} &= \begin{bmatrix} 1 & \xi \end{bmatrix} \\ \overline{\mathbf{X}} &= \begin{bmatrix} 1 & \xi & \xi^2 & \xi^3 \end{bmatrix} \\ \overline{\mathbf{X}_{,\xi}} &= \frac{1}{J} \cdot \frac{d\mathbf{X}}{d\xi} \end{aligned} \tag{B.2}$$

The variable ξ is the local coordinate and for a standard beam element can take a value of -1 and 1. From the polynomial vectors $\overline{\mathbf{X}}$ the a matrix $\mathbf{A}$ can be define evaluating the vectors $\overline{\mathbf{X}_i}$ for every value of ξ. Therefore the following matrices are obtained:

$$\mathbf{A}_{ax} = \begin{bmatrix} \overline{\mathbf{X}}_{ax}|_{-1} \\ \overline{\mathbf{X}}_{ax}|_{1} \end{bmatrix} \quad \mathbf{A}_{y} = \begin{bmatrix} \overline{\mathbf{X}}|_{-1} \\ \overline{\mathbf{X}}_{,\xi}|_{-1} \\ \overline{\mathbf{X}}|_{1} \\ \overline{\mathbf{X}}_{,\xi}|_{1} \end{bmatrix} \quad \mathbf{A}_{z} = \begin{bmatrix} \overline{\mathbf{X}}|_{-1} \\ \overline{\mathbf{X}}_{,\xi}|_{-1} \\ \overline{\mathbf{X}}|_{1} \\ \overline{\mathbf{X}}_{,\xi}|_{1} \end{bmatrix} \quad \mathbf{A}_{\phi} = \begin{bmatrix} \overline{\mathbf{X}}|_{-1} \\ \overline{\mathbf{X}}_{,\xi}|_{-1} \\ \overline{\mathbf{X}}|_{1} \\ \overline{\mathbf{X}}_{,\xi}|_{1} \end{bmatrix} \tag{B.3}$$

The shape functions vectors for the three displacement and the additional twisting angle, can be obtained as :

$$\overline{\mathbf{SH}}_{ax} = \mathbf{A}_{ax}^{-1}\ \overline{\mathbf{X}}_{ax}; \quad \overline{\mathbf{SH}}_{y} = \mathbf{A}_{y}^{-1}\ \overline{\mathbf{X}}; \quad \overline{\mathbf{SH}}_{z} = \mathbf{A}_{z}^{-1}\ \overline{\mathbf{X}}; \quad \overline{\mathbf{SH}_{\phi}} = \mathbf{A}_{\phi}^{-1}\ \overline{\mathbf{X}}; \tag{B.4}$$

The shape function matrices for the 14 d.o.f*s* beam element can be obtained placing at the right position the shape function corresponding with the interpolated d.o.f. The shape function matrix $\mathbf{N}$ has the dimension $[4 \times 14]$. it can be written in a reduced form as:

$$\mathbf{N} = \begin{bmatrix} \overline{\mathbf{N}}_{ax} \\ \overline{\mathbf{N}}_{y} \\ \overline{\mathbf{N}}_{z} \\ \overline{\mathbf{N}}_{\phi} \end{bmatrix} \tag{B.5}$$

Each one of the shape function vector as a dimension $[1 \times 14]$. From the matrix $\mathbf{N}$, the strain interpolation matrix $\mathbf{B}$ is obtain:

$$\mathbf{B} = \begin{bmatrix} \overline{\mathbf{N}}_{ax,x} \cdot J^{-1} \\ \overline{\mathbf{N}}_{y,xx} \cdot 2\ J^{-1} \\ \overline{\mathbf{N}}_{z,xx} \cdot 2\ J^{-1} \\ \overline{\mathbf{N}}_{\phi,xx} \cdot 2\ J^{-1} \end{bmatrix} \tag{B.6}$$

On the other hand, the rotation interpolation matrix matrix G can be written as:

$$\mathbf{G} = \begin{bmatrix} \mathbf{0} \\ \overline{\mathbf{N}}_{y,x} \cdot J^{-1} \\ \overline{\mathbf{N}}_{z,x} \cdot J^{-1} \\ \overline{\mathbf{N}}_{\phi,x} \cdot J^{-1} \end{bmatrix} = \begin{bmatrix} \mathbf{0} \\ \overline{\mathbf{G}}_{y} \\ \overline{\mathbf{G}}_{z} \\ \overline{\mathbf{G}}_{\phi} \end{bmatrix} \tag{B.7}$$

Bibliography

[Carlos Luis Badillo Bercebal, 2014] Carlos Luis Badillo Bercebal, E. A. . G. F. . G. K. (2014). *Advanced Design of Steel Structure*. Aalborg Universitet.

[Cook et al., 2007] Cook, R. D. et al. (2007). *Concepts and applications of finite element analysis*. John Wiley & Sons.

[Jesper Dencker Larsen, 2007] Jesper Dencker Larsen, P. R. J. (2007). *Stabilitet af rammekonstruktioner -Rapport-*. Aalborg Universitet Esbjerg.

[Poulsen, 1994] Poulsen, J. F. . P. N. (1994). *Stabilitet og Postbuckling af Pladekonstruktioner*. Technical University of Denmark, Department of Structural Engineering.

[Poulsen and Damkilde, 1998] Poulsen, P. N. and Damkilde, L. (1998). Direct determination of asymptotic structural postbuckling behaviour by the finite element method. *International journal for numerical methods in engineering*, 42(4):685–702.

[Rahman, 2009] Rahman, T. (2009). *A perturbation approach for geometrically nonlinear structural analysis using a general purpose finite element code*. TU Delft, Faculteit Lucht-en Ruimtevaart Techniek.